

MATURITY AND EQUIVALENT AGE FUNCTIONS OF MINERAL  
ADMIXTURES INCORPORATED MORTARS

A THESIS SUBMITTED TO  
THE GRADUATE SCHOOL OF NATURAL AND APPLIED SCIENCES  
OF  
MIDDLE EAST TECHNICAL UNIVERSITY

BY  
MUHAMMET ATASEVER

IN PARTIAL FULFILLMENT OF THE REQUIREMENTS  
FOR  
THE DEGREE OF MASTER OF SCIENCE  
IN  
CIVIL ENGINEERING

May 2017



Approval of thesis:

**MATURITY AND EQUIVALENT AGE FUNCTIONS OF MINERAL  
ADMIXTURES INCORPORATED MORTARS**

Submitted by **MUHAMMET ATASEVER** in partial fulfillment of the requirements  
for the degree of **Master of Science in Civil Engineering Department, Middle  
East Technical University** by,

Prof. Dr. Gülbin Dural Ünver  
Dean, Graduate School of **Natural and Applied Sciences** \_\_\_\_\_

Prof. Dr. İsmail Özgür Yaman  
Head of Department, **Civil Engineering** \_\_\_\_\_

Prof. Dr. Mustafa Tokyay  
Supervisor, **Civil Engineering Dept., METU** \_\_\_\_\_

**Examining Committee Members**

Prof. Dr. Kambiz Ramyar  
Civil Engineering Dept., Ege University \_\_\_\_\_

Prof. Dr. Mustafa Tokyay  
Civil Engineering Dept., METU \_\_\_\_\_

Prof. Dr. İsmail Özgür Yaman  
Civil Engineering Dept., METU \_\_\_\_\_

Assoc. Prof. Dr. Sinan Turhan Erdoğan  
Civil Engineering Dept., METU \_\_\_\_\_

Prof. Dr. Mustafa Şahmaran  
Civil Engineering Dept., Hacettepe University \_\_\_\_\_

**Date: 26 May, 2017**

**I hereby declare that all information in this document has been obtained and presented in accordance with rules and ethical conduct. I also declare that as required by these rules and conduct, I have fully cited and referenced all material and results that are not original to this work.**

Name, Last name: Muhammet Atasever

Signature :

## **ABSTRACT**

### **MATURITY AND EQUIVALENT AGE FUNCTIONS OF MINERAL ADMIXTURES INCORPORATED MORTARS**

Atasever, Muhammet  
M.S., Department of Civil Engineering  
Supervisor: Prof. Dr. Mustafa Tokyay

May 2017, 99 Pages

There are many studies on the maturity method, which is a non-destructive testing methods. However, most of these studies are associated with portland cement and its types. In this study, 4 different mineral admixtures (limestone powder, trass, fly ash and ground granulated blast furnace slag) were used at 6%, 20% and 35% (by mass) replacement levels. Besides the control portland cement mortars, mortars having  $110 \pm 5\%$  flow according to ASTM C109 were also prepared using the blended cements. Then, 2, 7, 14, 28 and 90-day compressive strengths of 13 different mortars were determined.

The aim of this thesis is to investigate the effects of mineral admixture type and amount on the maturity and equivalent age functions using methods described in the relevant standard (ASTM C1074). For this purpose, apparent activation energy and datum temperature of these 13 mixtures were determined according to 3 different options in ASTM C1074 and these options were examined. In addition, a new

approach was proposed especially for blended cements by using Option A1.1.8.1. and the results obtained from this approach were discussed in detail. In addition, a method was proposed for the determination of apparent activation energy and datum temperature by considering the compressive strength-age relationship of these mixtures. Besides, the relationship between the Nurse-Saul equivalent age function and ratio of compressive strength at 3 different curing temperature by taking the reference temperature as 20°C was examined.

**Keywords:** maturity, apparent activation energy, datum temperature, equivalent age functions, strength development.

## ÖZ

### **MİNERAL KATKI İÇEREN HARÇLARIN OLGUNLUK VE EŞDEĞER YAŞ FONKSİYONLARI**

Atasever, Muhammet  
Yüksek Lisans, İnşaat Mühendisliği Bölümü  
Tez Yöneticisi: Prof. Dr. Mustafa Tokyay

Mayıs 2017, 99 Sayfa

Tahribatsız muayene metotlarından biri olan olgunluk metodu üzerine birçok çalışma vardır. Ancak bu çalışmaların çoğu portland çimentosu ve çeşitleri ile ilişkilidir. Bu çalışmada, 4 farklı mineral katkı çimento yerine (kalker tozu, tras, uçucu kül ve öğütülmüş yüksek fırın cürufu) kütlece %6, %20 ve %35 oranlarında kullanılmıştır. Kontrol portland çimentosu ile üretilen harçlara ilaveten, katkılı çimentolarla ASTM C109'a göre  $110 \pm 5\%$  yayılma değerine sahip harçlar da hazırlanmıştır. Daha sonra, 13 farklı harcın 2, 7, 14, 28 ve 90 günlük basınç dayanımları belirlenmiştir.

Bu tezin amacı, mineral katkı çeşidinin ve miktarının olgunluk ve eşdeğer yaş fonksiyonlarına etkisini ilgili standartta (ASTM C1074) belirtilen yöntemleri kullanılarak incelemektir. Bu amaç için, karışımların, zahiri aktivasyon enerjisi ve baz sıcaklığı, ASTM C1074'te yer alan 3 farklı yönteme göre belirlenmiş ve bu yöntemler irdelenmiştir. Ayrıca, ASTM C1074'te yer alan A1.1.8.1 seçeneği kullanılarak, özellikle mineral katkılı çimentolar için, zahiri aktivasyon enerjisi ve baz sıcaklığının belirlenmesinde yeni bir yaklaşım önerilmiş ve bu yaklaşımdan elde edilen sonuçlar detaylıca tartışılmıştır. Bunlara ilaveten, bu karışımların basınç dayanımı-yaş ilişkisi

dikkate alınarak, zahiri aktivasyon enerjisinin ve baz sıcaklığının belirlenmesi için bir yöntem önerilmiştir. Ayrıca, referans sıcaklığını 20°C kabul ederek, Nurse-Saul eşdeğer yaş fonksiyonu ve 3 farklı sıcaklıktaki basınç dayanım oranları arasındaki ilişki incelenmiştir.

**Anahtar Kelimeler:** olgunluk, zahiri aktivasyon enerjisi, baz sıcaklığı, eşdeğer yaş fonksiyonları, dayanım gelişimi



*To My Beloved Daughter*

*Duru*

## ACKNOWLEDGEMENTS

First and foremost, I would like to express my gratitude to my thesis advisor, Prof. Dr. Mustafa Tokyay, for his endless assistance, suggestions and guidance throughout this research. Also, I would like to thank him for his encouragement by making insightful discussions with me during the preparation of this thesis.

I also want to thank Assoc. Prof. Dr. Sinan Turhan Erdoğan and Prof. Dr. İsmail Özgür Yaman for their valuable advice and help during my experiments.

I wish to thank Prof. Dr. Kambiz Ramyar and Prof. Dr. Mustafa Şahmaran whose helped to improve the quality of this thesis.

I would like to thank the staff and my colleagues in the Division of Materials of Construction in METU, Cuma Yıldırım, Gültekin Ozan Uçal, Murat Şahin, Dr. Burhan Aleessa Alam, Mehmet Kemal Ardoğa, Meltem Tangüler Bayramtan, Özgür Paşaoğlu and Mehran Ghasabeh for their kind help during my master's study.

I would like to pay sincere and heartiest thanks my parents, Süheyla and Prof. Dr. Mustafa Atasever, my sister, Aybüke, and my brother, Ömer Mert for all their never-ending love and encouragement no matter what path I choose through my whole life.

I would also like to thank my wife, İlknur, for always being there for me, and her moral support, endurance and patience during the study. This last word of the acknowledgement I have saved for my baby girl, Duru, who has given me much happiness, for being such a sweet baby and cheering me up.

## TABLE OF CONTENTS

ABSTRACT.....	v
ÖZ .....	vii
ACKNOWLEDGEMENTS .....	x
TABLE OF CONTENTS.....	xi
LIST OF TABLES .....	xv
LIST OF FIGURES .....	xvi
LIST OF ABBREVIATIONS .....	xix
CHAPTERS	
1. INTRODUCTION .....	1
1.1. General.....	1
1.2. Objective and Scope .....	2
2. BACKGROUND OF MATURITY METHOD .....	5
2.1. Development of the Maturity Method .....	5
2.2. Strength and Maturity Relations .....	9
2.3. Determination of Apparent Activation Energy and Datum Temperature....	11
3. MINERAL ADMIXTURES .....	15
3.1. General.....	15
3.1.1. Trass.....	18
3.1.2. Limestone.....	18
3.1.3 Fly Ash.....	18
3.1.4. Blast Furnace Slag (BFS) .....	21
3.2. Influence of Mineral Admixtures on Hydration .....	21
3.2.1. Physical Influence.....	21

3.2.2. Chemical Influence .....	22
4. REVIEW OF RECENT RESEARCH.....	25
5. EXPERIMENTAL PROGRAM .....	35
5.1. Materials .....	35
5.1.1. Cement and Mineral Admixtures.....	35
5.1.2. Standard Sand .....	36
5.1.3. Water.....	36
5.1.4. Mixture Proportions .....	36
5.2. Test Methods.....	37
5.2.1. Tests on Pastes .....	37
5.2.1.1. Normal Consistency and Setting Time Tests.....	37
5.2.2. Tests on Mortars .....	38
5.2.2.1. Mixing and Moulding Procedure .....	38
5.2.2.2. Flow Test .....	38
5.2.2.3. Compressive Strength .....	38
5.3. Curing Conditions.....	39
6. DISCUSSION AND RESULTS .....	41
6.1. Analysis of Data Based on ASTM C1074 Methods .....	43
6.2. Strength Development and Nurse-Saul Maturity Function .....	48
6.3. A New Approach for Examination of Datum Temperature and Apparent Activation Energy .....	63
6.4. Development of A New Method for the Determination of Datum Temperature and Apparent Activation Energy .....	66
6.5. Equivalent Age Functions.....	68
7. CONCLUSIONS .....	75
REFERENCES.....	77
APPENDICES	

APPENDIX A .....	83
A1. Determination of Datum Temperature and Apparent Activation Energy According to Option A1.1.7.....	83
A2. Determination of Datum Temperature and Apparent Activation Energy According to Option A1.1.8.1.....	86
A3. Determination of Datum Temperature and Apparent Activation Energy According to Option A1.1.8.2.....	88
APPENDIX B .....	93
APPENDIX C .....	96

## LIST OF TABLES

### TABLES

Table 3.1 Comprasion of fly ashes classified according to their chemical properties	20
Table 5.1 Chemical and physical properties of materials used .....	36
Table 5.2 Mortar mix proportions .....	37
Table 6.1 Compressive strength test results .....	41
Table 6.2 $T_0$ and $E_a$ values according to the proposed approach.....	44
Table 6.3 Initial - final setting times 20°C and w/c required to normal consistency for each mixtures.....	45
Table 6.4 Coefficients of determination of experimental strength vs. maturity for each type of mixture .....	48
Table 6.5 Slope values of experimental strength vs. predicted strength for each type of mixtures.....	49
Table 6.6 $T_0$ and $E_a$ values for each type of mixtures according to the new approach .....	65
Table 6.7 $T_0$ and $E_a$ values for each type of mixtures according to proposed method .....	68
Table A.1 Experimental compressive strength test results and age beyond final setting time for Control specimens.....	83
Table A.2 Reciprocal age beyond final setting time and reciprocal experimental compressive strength results for Control specimens .....	84
Table A.3 k-values at each temperature in Option A1.1.7 for Control specimens ....	85
Table A.4 Reciprocal curing temperature and natural logarithm of k-values for Control specimens .....	85
Table A.5 $S_u$ , $k_T$ , and $t_0$ values at each temperatures for Control specimens.....	87
Table A.6 $S_u$ values at each temperatures for Control specimens .....	89
Table A.7 A-values for first four test ages at three different temperatures for Control specimens .....	90
Table A.8 k-values at each curing temperatures in Option A1.1.8.2 for Control specimens .....	91

Table A.9 Reciprocal curing temperature and natural logarithm of k-values for Control specimens.....	92
Table C.1 Compressive strength test results and reciprocal natural logarithm of age beyond final setting time at 20°C for Control specimens .....	96
Table C.2 Reciprocal natural logarithm of age beyond final setting time at 20°C and reciprocal experimental compressive strength results for Control specimens .....	96
Table C.3 T-values at each of temperatures in the proposed method for Control specimens .....	97
Table C.4 Reciprocal curing temperature and natural logarithm of T-values for Control specimen .....	98

## LIST OF FIGURES

### FIGURES

Figure 2.1 Age conversion factor-concrete temperature plots for different activation energies (adopted from Fig. 3 of Carino and Lew (2001)) .....	9
Figure 2.2 Schematic representation of maturity method .....	12
Figure 3.1 Classification of pozzolans (Massazza, 1988) .....	17
Figure 6.1 (a) Experimental strength-age (b) Experimental strength-maturity relationships for Control specimens .....	50
Figure 6.2 (a) Experimental strength-age (b) Experimental strength-maturity relationships for LS-6 specimens .....	51
Figure 6.3 (a) Experimental strength-age (b) Experimental strength-maturity relationships for LS-20 specimens .....	52
Figure 6.4 (a) Experimental strength-age (b) Experimental strength-maturity relationships for LS-35 specimens .....	53
Figure 6.5 (a) Experimental strength-age (b) Experimental strength-maturity relationships for T-6 specimens .....	54
Figure 6.6 (a) Experimental strength-age (b) Experimental strength-maturity relationships for T-20 specimens .....	55
Figure 6.7 (a) Experimental strength-age (b) Experimental strength-maturity relationships for T-35 specimens .....	56
Figure 6.8 (a) Experimental strength-age (b) Experimental strength-maturity relationships for FA-6 specimens .....	57
Figure 6.9 (a) Experimental strength-age (b) Experimental strength-maturity relationships for FA-20 specimens .....	58
Figure 6.10 (a) Experimental strength-age (b) Experimental strength-maturity relationships for FA-35 specimens .....	59
Figure 6.11 (a) Experimental strength-age (b) Experimental strength-maturity relationships for S-6 specimens .....	60
Figure 6.12 (a) Experimental strength-age (b) Experimental strength-maturity relationships for S-20 specimens .....	61



Figure 6.13 (a) Experimental strength-age (b) Experimental strength-maturity relationships for S-35 specimens .....	62
Figure 6.14 Strength development rate for mortars without mineral admixtures .....	67
Figure 6.15 Relative strength-equivalent age for Control specimens .....	69
Figure 6.16 Relative strength-equivalent age for LS-6 specimens .....	70
Figure 6.17 Relative strength-equivalent age for LS-20 specimens .....	70
Figure 6.18 Relative strength-equivalent age for LS-35 specimens .....	70
Figure 6.19 Relative strength-equivalent age for T-6 specimens .....	71
Figure 6.20 Relative strength-equivalent age for T-20 specimens .....	71
Figure 6.21 Relative strength-equivalent age for T-35 specimens .....	71
Figure 6.22 Relative strength-equivalent age for FA-6 specimens .....	72
Figure 6.23 Relative strength-equivalent age for FA-20 specimens .....	72
Figure 6.24 Relative strength-equivalent age for FA-35 specimens .....	72
Figure 6.25 Relative strength-equivalent age for S-6 specimens .....	73
Figure 6.26 Relative strength-equivalent age for S-20 specimens .....	73
Figure 6.27 Relative strength-equivalent age for S-35 specimens .....	73
Figure A.1 Reciprocal of experimental strength vs. reciprocal of age beyond time of final setting for Control specimens in Option A1.1.7 .....	84
Figure A.2 $k$ -values vs. curing temperature for Control specimens in Option A1.1.7 .....	85
Figure A.3 Natural logarithm of $k$ -values vs. inverse absolute temperature for Control specimens in Option A1.1.7 .....	86
Figure A.4 $k_T$ -values vs. curing temperature for Control specimens in Option A1.1.8.1 .....	87
Figure A.5 Natural logarithm of $k$ -values vs. inverse absolute temperature for Control specimens in Option A1.1.8.1 .....	88
Figure A.6 Reciprocal of strength vs. reciprocal of age for Control specimens in Option A1.1.8.2 .....	89
Figure A.7 Reciprocal of strength vs. reciprocal of age for Control specimens in Option A1.1.8.2 .....	90
Figure A.8 Reciprocal of strength vs. reciprocal of age for Control specimens in Option A1.1.8.2 .....	91

Figure A.9 Natural logarithm of k-values vs. inverse absolute temperature for Control specimens in Option A1.1.8.2 .....	92
Figure B.1 Experimental strength vs. predicted strength for Control specimens .....	93
Figure B.2 Experimental strength vs. predicted strength for (a) LS-6, (b) LS-20, (c) LS-35, (d) T-6, (e) T-20, (f) T-35 specimens .....	94
Figure B.3 Experimental strength vs. predicted strength for (a) FA-6, (b) FA-20, (c) FA-35, (d) S-6, (e) S-20, (f) S-35 specimens .....	95
Figure C.1 Reciprocal of experimental strength vs. reciprocal reciprocal natural logarithm of age beyond final setting time at 20°C for Control specimens .....	97
Figure C.2 T-values vs. curing temperature for Control specimens in the proposed method .....	98
Figure C.3 Natural logarithm of T-values vs. inverse absolute temperature for Control specimens in the proposed method .....	99

## LIST OF ABBREVIATIONS

ASTM	:	American Society for Testing and Materials
EN	:	European Norm
TCMA	:	Turkish Cement Manufacturers' Association
ACI	:	American Concrete Institute
GGBFS	:	Ground Granulated Blast Furnace Slag
Control	:	Control Portland Cement
T-6	:	6% Trass-Blended Cement
T-20	:	20% Trass-Blended Cement
T-35	:	35% Trass-Blended Cement
LS-6	:	6% Limestone-Blended Cement
LS-20	:	20% Limestone-Blended Cement
LS-35	:	35% Limestone-Blended Cement
FA-6	:	6% Fly Ash-Blended Cement
FA-20	:	20% Fly Ash-Blended Cement
FA-35	:	35% Fly Ash-Blended Cement
S-6	:	6% Ground Granulated Blast Furnace Slag-Blended Cement
S-20	:	20% Ground Granulated Blast Furnace Slag-Blended Cement
S-35	:	35% Ground Granulated Blast Furnace Slag-Blended Cement
$T_0$	:	Datum Temperature
$E_a$	:	Apparent Activation Energy
S	:	SiO <sub>2</sub>
A	:	Al <sub>2</sub> O <sub>3</sub>
F	:	Fe <sub>2</sub> O <sub>3</sub>
C	:	CaO
$\bar{S}$	:	SO <sub>3</sub>



## **CHAPTER 1**

### **INTRODUCTION**

#### **1.1. General**

There are three preparation phases for concrete casting to produce concrete compatible with related specifications in construction site: before, during and after the mixing. The first is mainly associated with concrete mix design (i.e, proportioning of concrete mixes), transporting of fresh concrete providing relevant specifications, guaranteeing safety of workers, and jobsharing among them. The second is correct handling, placing with proper compaction and finishing of concrete, and the last is curing of concrete by choosing one of proper curing methods, and removal of concrete forms when the concrete reaches sufficient strength to carry loads acting on the structural member.

Concrete properties progress with time as long as the ambient temperature and humidity are favorable for the hydration of cement. Therefore, curing of concrete which may be defined as “the actions taken to maintain moisture and temperature condition in a freshly-placed cementitious mixture to allow hydraulic-cement hydration and (if applicable) pozzolanic reactions to occur so that the potential properties of the mixture may develop (ASTM C125, 2003) is an essential point of any concrete-making process.

American Concrete Institute (ACI) describes curing as the process through which the concrete matures and develops hardened properties with time with appropriate humidity and temperature (ACI 308, 2001).

One of the major decisions taken during a concrete construction is the time of removal of formwork which requires a reasonable prediction of in-place strength of concrete. Furthermore, processes like post-tensioning, stopping the cold weather protection, opening a road to traffic and transportation of prefabricated elements require adequate strength prediction, also. In other words, application and scheduling of various critical processes during concrete construction can be made properly when the concrete attains a sufficient strength for the purpose for which it is made (Kasap, 2002). The maturity method is a means of estimating the combined effect of time and temperature during the curing process on the development of concrete properties, especially the strength. The maturity method is based on the effect of temperature on the rate of hydration of cement. Since the process involves a series of chemical reactions between cement components and water, the higher the temperature, the more rapid will the hydration be, and therefore, strength and other relevant properties will more rapidly develop. Concrete matures as degree of hydration of cement increases (ACI 308, 2001). There have been several methods developed to estimate or predict the strength of concrete in relation with its age and curing temperature history. Among them, the Nurse-Saul maturity function and the equivalent age function are the ones that received general acceptance. These two methods have become standard practice for estimating concrete strength since 1974 (ASTM C1074, 2011).

## **1.2. Objective and Scope**

The use of mineral admixtures in concrete either as a constituent of blended cements or as an ingredient of concrete mixes has been a common practice since 1990s. Their effect on the properties of concrete have long been the subject matter of a vast amount of research. On the other hand, the maturity and equivalent age functions which were originally developed for portland cement concretes, and were not yet studied thoroughly for mineral admixture-incorporated concretes or concretes made by using blended cements.

The aim of this experimental study is to determine the effects of mineral admixture type and amount on the maturity of concrete and applicability of the maturity and equivalent age functions described in the relevant standard (ASTM C1074) to blended cement concretes.

For this purpose, besides the control portland cement specimens without any mineral admixtures, a natural pozzolan, a ground limestone, a low-lime fly ash and a GGBFS were used to replace 6, 20 and 35% (by mass) portland cement and mortar specimens were prepared. The specimens were moist cured at 5°C, 20°C and 40°C and compressive strength tests were carried out at 2, 7, 14, 28, 90-day. Finally, the results obtained were analysed from maturity and equivalent age points of view, in comparison with the control portland cement mortars.





## CHAPTER 2

### 2 BACKGROUND OF MATURITY METHOD

#### 2.1. Development of the Maturity Method

The concept that there is a correlation between strength and age-temperature due to hydration reactions was firstly proposed by McIntosh (1949). He brought forward idea of “basic age” to draw an analogy between non-conductive concrete samples and concrete samples exposed to electrical current. He introduced the threshold temperature, datum, for hardening of concrete as 30°F (-1 °C). However, he remained insufficient while making assumptions concerned with “basic age”. Therefore, he suggested some indexes such as the heating index,  $I_h$ , and the strength index,  $I_s$ , which are defined as follows:

$$I_h = \frac{\text{basic age of heated specimen}}{\text{basic age of corresponding control specimen to give strength equal to that of the heated specimen}} \quad (2.1)$$

$$I_s = \frac{\text{strength of heated specimen}}{\text{strength of control specimen at a basic age equal to [basic age of heated specimen} \times \text{a factor]}} \quad (2.2)$$

Nurse (1949) was also interested in the combined effect of time and temperature on strength of concrete. His study was basically on the effect of steam curing on strength development. Both of the studies mentioned above were related with accelerated curing of concrete.

Later on, the idea was used for the strength development under conventional curing conditions and the term “maturity” was first proposed by Saul (1951). The famous Nurse-Saul Maturity Function was described as follows:

$$M = \sum_0^t (T - T_0) \cdot \Delta t \quad (2.3)$$

where,

$M$ : Maturity index at age  $t$ , [degree-days or degree-hours],

$T$ : Average concrete temperature during the time interval,  $\Delta t$ , [ $^{\circ}\text{C}$ ],

$T_0$  : Datum temperature [ $^{\circ}\text{C}$ ], and

$\Delta t$  : A time interval [days or hours].

Equation (2.3) assumes that early rate of strength development is linearly related to temperature. However, it was analyzed that the linear approximation may not be true for wide ranges of temperature-time. In other words, the linear relationship between rate of strength development and temperature is only applicable to concretes with  $T_0$  about  $-10^{\circ}\text{C}$  and cured at temperatures around  $20^{\circ}\text{C}$  (Bergstrom, 1953). In order to overcome this deficiency of Nurse-Saul maturity function several alternative functions were proposed, but none of them received much acceptance (Carino and Lew, 2001).

Rastrup (1954) was the first to propose an equivalent age function based on the increase in rate of the hydration as the temperature increases. The function enabled to compare the age at a known constant temperature with the age at any randomly chosen temperature:

$$t_e = \int_0^t 2^{((T-T_r)/10)} dt \quad (2.4)$$

where,

$t_e$  : Equivalent age [days or hours],

$T$  : Average concrete temperature during the time interval,  $\Delta t$ , [°C],

$T_r$  : Reference temperature [°C].

He also compared the proposed equation with Nurse-Saul maturity value as follows:

$$t_e = \sum \alpha \cdot \Delta t \quad (2.5)$$

or

$$t_e = \sum \left( \frac{T - T_0}{T_r - T_0} \right) \cdot \Delta t \quad (2.6)$$

where,

$t_e$  : Equivalent age [days or hours]

$\alpha$  : Age conversion factor,

$T$  : Average concrete temperature during the time interval,  $\Delta t$ , [°C],

$T_r$  : Reference temperature [°C],

$T_0$  : Datum temperature [°C], and

$\Delta t$  : A time interval [days or hours].

He specified that conformity between Equation (2.4) and Equation (2.6) was valid only for temperatures below 20-25°C.

Hansen and Pedersen (1977) proposed a new equivalent age function based on the Arrhenius equation:

$$t_e = \sum_0^t e^{-\frac{E_a}{R} \left( \frac{1}{T} - \frac{1}{T_r} \right)} \cdot \Delta t \quad (2.7)$$

For  $T \geq 20^\circ\text{C}$       $E_a = 33\,500 \text{ J/mol}$

For  $T < 20^\circ\text{C}$       $E_a = 33\,500 + 1470 [20 - T] \text{ J/mol}$

where,

$t_e$  : Equivalent age [days or hours]

$E_a$  : Apparent activation energy, [J/mol]

$R$  : Gas constant, [8.314 J/mol-°K]

$T$  : Average concrete temperature during the time interval,  $\Delta t$ , [°K],

$T_r$  : Reference temperature [°K],

$\Delta t$  : A time interval [days or hours].

Equation (2.7) overcomes the limitation of Nurse-Saul function by allowing a non-linear relationship between the initial rate of strength gain and temperature. Besides, the formula can be used for a wider temperature range if  $E_a$  is assigned correctly. The significance of assigning the appropriate  $E_a$  in Equation (2.7) was explained as follows: The exponential term in the equation converts time increment at the actual concrete temperature to equivalent time increment at a reference temperature. Therefore, it can be named the age conversion factor ( $\gamma$ ). When  $\gamma$  is plotted against concrete temperature for different  $E_a$  values in Figure 2.1, for lower  $E_a$  values, the relationship may be assumed as linear whereas for higher  $E_a$  values, there is a high nonlinearity. Thus, it can be seen that if an appropriate  $E_a$  is not used, Equation (2.7) may be misleading (Carino and Lew, 2001).

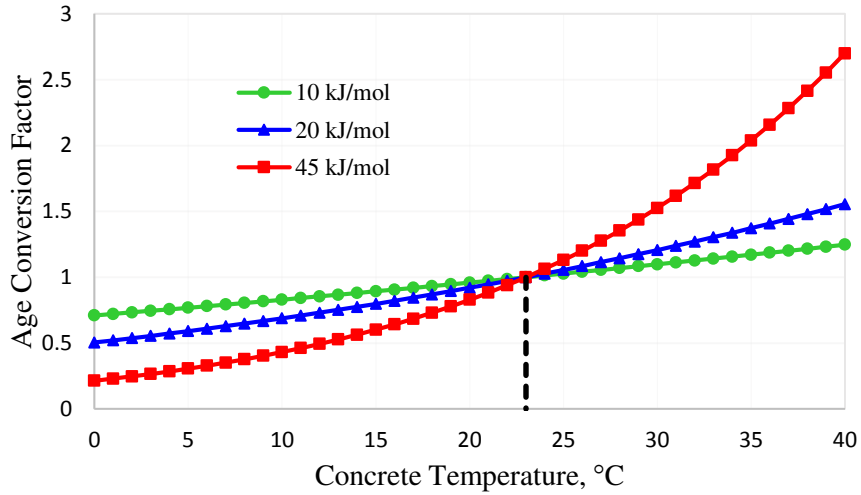


Figure 2.1 Age conversion factor-concrete temperature plots for different activation energies (adopted from Fig. 3 of Carino and Lew (2001))

## 2.2. Strength and Maturity Relations

After determination of maturity, it is required to establish the maturity-strength relationship. Several functions have been proposed for this relationship. One of the first such relationships was suggested by Plowman (1956). He analyzed maturity-compressive strength relationship, valid at constant temperatures, by using Equation (2.8),

$$S = a + b \cdot \log(M) \quad (2.8)$$

where,

$S$  : Compressive strength [0.0068 · MPa],

$a$  and  $b$  : Constants,

$M$  : Maturity index [°C – hr].

According to him, Equation (2.8) does not depend on cement type, the curing temperature, or the specimen's geometrical form (i.e. cube or cylinder). Besides, four strength classifies were adequate to estimate  $a$  and  $b$  values. In spite of these

assumptions, the logarithmic function can be chosen due to its simplicity.

Carino (1997) used the following hyperbolic function with three variables ( $S_u$ ,  $k_T$  and  $t_0$ ).

$$S = S_u \cdot \frac{k_T \cdot (t - t_0)}{1 + k_T \cdot (t - t_0)} \quad (2.9)$$

where,

$S$  : Compressive strength at age  $t$ , [days],

$S_u$  : Ultimate strength,

$k_T$  : Rate constant,  $[1/\text{days}]$

$t_0$  : Age at start of strength development, [days].

As Carino mentioned, the approach assumes that the strength evolution begins at an age after the final setting time, and this age can be taken as the inverse of the rate constant to obtain the point where strength is half of ultimate strength. To solve the equation, the least squares method is employed on the strength-age curve. Actually ultimate strength of concrete cured at a certain temperature basically can be defined as its strength at infinite age cured at the same temperature.

A similar model was proposed by Knudsen (1980) assuming a parabolic relationship between time and rate constant.

$$S = S_u \cdot \frac{\sqrt{k_T \cdot (t - t_0)}}{1 + \sqrt{k_T \cdot (t - t_0)}} \quad (2.10)$$

where,

$S$  : Compressive strength at age  $t$ , [days],

$S_u$  : Ultimate strength,

$k_T$  : Rate constant,

$t_0$  : Age at start of strength development, [days].

In Equation (2.9), degree of hydration of particles in cementitious systems was taken as a linear function of time-rate constants. Thus, Equation (2.9) can be named linear hyperbolic function, while Equation (2.10) is called parabolic hyperbolic due to its square root terms.

Hansen and Pedersen (1977) proposed the following equation for the strength-maturity relationship:

$$S = S_u \cdot e^{-\left(\frac{N}{t}\right)^\alpha} \quad (2.11)$$

where,

t : Age

N : A constant [representing the age at which the strength reached  $0.37S_u$ ]

$\alpha$  : A shape parameter (related with the slope of the curve during the early periods of strength gain).

It was shown experimentally that Equation (2.9) is applicable up to 28-day, Equation (2.10) is suitable for later ages, and Equation (2.11) fits for all ages (Hansen and Pedersen, 1977).

### **2.3. Determination of Apparent Activation Energy and Datum Temperature**

Activation energy can be defined as the minimum energy required to initiate any chemical reaction among the molecules. (Shukla and Mishra, 2015).

The definition is also valid for cement hydration as any exothermic reaction, yet a narrower definition is necessary to understand its significance for maturity method. Thus,  $E_a$  in the maturity method is a minimum energy for concrete to gain strength.

“ $T_0$ , on the other hand, may be defined as the lowest temperature at which the concrete will not gain strength” (Nixon et al., 2008).

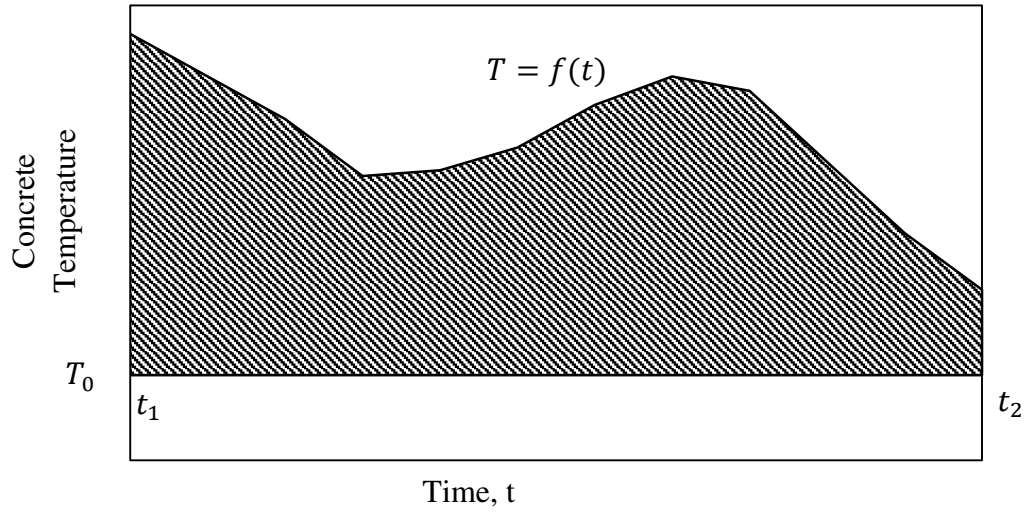


Figure 2.2 Schematic representation of the maturity method

If Nurse-Saul maturity function is derived mathematically as the set of data from Figure 2.2,

$$T = f(t) \quad (2.12)$$

Taking the integral from  $t_1$  to  $t_2$  of both sides,

$$\int_{t_1}^{t_2} T \, dt = \int_{t_1}^{t_2} f(t) \, dt \quad (2.13)$$

$$T \cdot t \Big|_{t_1}^{t_2} + c = F(t) \Big|_{t_1}^{t_2} + c \quad (2.14)$$

$$T(t_2 - t_1) = F(t_2) - F(t_1) \quad (2.15)$$

$$\int_{t_1}^{t_2} f(t) \, dt = T \cdot (t_2 - t_1) \quad (2.16)$$



The area under the curve,

$$M = \int_{t_1}^{t_2} f(t) dt - T_0 \cdot (t_2 - t_1) \quad (2.17)$$

Since  $\int_{t_1}^{t_2} f(t) dt = T \cdot (t_2 - t_1)$  from Equation (2.16),

$$M = T \cdot (t_2 - t_1) - T_0 \cdot (t_2 - t_1) \quad (2.18)$$

$$M = (T - T_0) \cdot (t_2 - t_1) \quad (2.19)$$

Actually, taking  $(t_2 - t_1) = \Delta t$ , Equation (2.3) is obtained.

Owing to the difficulty of establishing a common maturity-strength relationship for all types of concrete because of the nature of concrete, especially mineral admixture-incorporated concrete, employment of accurate  $E_a$  and  $T_0$  values for relevant maturity functions becomes crucial. Thus, Malhotra and Carino (2004) suggested some methods for identification of activation energy such as by chemical shrinkage, by heat of hydration or by strength tests of mortar or concrete even though there is not a known way to determine  $T_0$  except for the method stated in ASTM C1074.

ASTM C1074 (2011) allows three different options to determine  $E_a$  and  $T_0$ :

1. After plotting the reciprocal of strength vs. reciprocal of age beyond final setting times, values of intercept divided by slope for each straight-line gives rate constants. (Option A1.1.7 in ASTM C1074)
2. Unless final setting times are measured, rate constants can be determined by solving Equation (2.9) for three curing temperatures, and changing the variables ( $S_u$ ,  $k_T$ , and  $t_0$ ) in Equation (2.9) (Option A1.1.8.1 in ASTM C1074).
3. Plotting reciprocal of strength vs. reciprocal of age, inverse of the intercept at y-axis gives  $S_u$ . This is repeated for each of the three curing temperature. Then, plotting A vs. age by using following equation and slopes for each straight-line for each curing temperature give rate constants. (Option A1.1.8.2 in ASTM C1074)

$$A = \frac{S}{(S_u - S)} \quad (2.20)$$

After determining k-values or rate constants by one of the stated methods, no matter which method is used, the following procedure was applied for calculation of  $T_0$  and  $E_a$  in the thesis:

In computing  $E_a$ , after natural logarithms of rate constants were calculated, and three different curing temperatures with [ $^{\circ}\text{C}$ ] were converted to [ $^{\circ}\text{K}$ ], a straight line with negative slope was obtained.  $E_a$  was obtained by multiplying the slope (in absolute value) by the gas constant, R.

In calculating  $T_0$ , providing that rate constants along the y-axis and curing temperature along the x-axis, a straight line was plotted. Then the intercept of the line with x-axis is determined. This point was  $T_0$ .

## CHAPTER 3

### 3 MINERAL ADMIXTURES

#### 3.1. General

Mineral admixtures are inorganic mineral substances (or material) incorporated into concrete in finely divided form and usually in large amounts. They may be used to partially replace form for portland cement and/or fine aggregate as a main ingredient of concrete.

Mineral admixtures affect almost every property of concrete into which they are incorporated, both in fresh and hardened states. Technically speaking, the main idea behind using mineral admixtures in concrete is to improve the workability of fresh concrete and the durability of hardened concrete. Besides the technical aspect, there are economical and ecological aspects of using mineral admixtures, too. Reduction in the energy consumption in cement manufacturing is one of them. About 30% of the total cost of cement in the energy requirement and the two most important energy consuming processes in cement manufacturing are (1) the burning processes in the rotary kiln and (2) comminution (crushing and grinding). Most of the mineral admixtures do not require a burning process and they are either softer than portland cement clinker and therefore easier to grind or they are already in sufficiently fine particulate form. Thus, their use reduces the energy consumption. Furthermore, the burning process in the rotary kiln results in approximately 0.9 kg of CO<sub>2</sub> emissions per kg of clinker produced. About 1/3 of it is due to carbon based fuels and about 2/3 is

given off through the calcination of raw materials, basically the limestone (Gartner, 2004; CSI, 2005; Damtoft et al., 2008). Thus, using mineral admixtures to partially replace the portland cement in concrete would lead to considerable reduction in greenhouse gas emissions.

Mineral admixtures may be grouped into three broad categories as (1) materials of low or no reactivity which include ground limestone, dolomite, quartz and hydrated lime; (2) pozzolans which are siliceous or siliceous and aluminous materials that possess very little or no cementitious value by themselves but react with calcium hydroxide under moist conditions to form compounds with binding value; (3) latent hydraulic materials which have the ability to form cementitious products after reacting with water. The materials in the first category are mainly used to adjust the workability. Concretes that are deficient in fine aggregate are susceptible to segregation and bleeding. Therefore, incorporation of mineral admixtures like ground limestone would improve the cohesiveness of the fresh concrete by increasing the fines content (Tokyay, 2016).

Pozzolanic materials which are comprised in the second category have the ability to react with calcium hydroxide, in the presence of water, to form C-S-H and calcium aluminate hydrates with binding value. The reactions leading to the formation of these hydrates are named pozzolanic reactions. Pozzolanic reactions require pozzolan to be amorphous in nature and in pulverized form. These reactions are almost always gradual.

There are many siliceous or siliceous and aluminous materials with pozzolanic properties. A comprehensive classification of pozzolans is given in Figure 3.1

Latent hydraulic materials of the third category are GGBFS and high-lime fly ash (HLFA). Blast furnace slag is a by-product of pig iron production. It is obtained from the blast furnace in molten form. It should be cooled rapidly in order to be used as a mineral admixture in concrete. The crystalline content of a suitable GGBFS is usually

less than 5% and the glassy phase is mainly composed of silicate with calcium, magnesium, and aluminium ions (Moranville-Regourd, 1988). Blast furnace slag should be ground to cement fineness in order to be used in concrete.

High-lime fly ashes are the by-product of thermal power plants burning lignitic and subbituminous coals. Their glassy phase consist of silicate with calcium, magnesium, aluminium, and alkali ions (Mehta and Monteiro, 2006; Alonso and Wesche 1991).

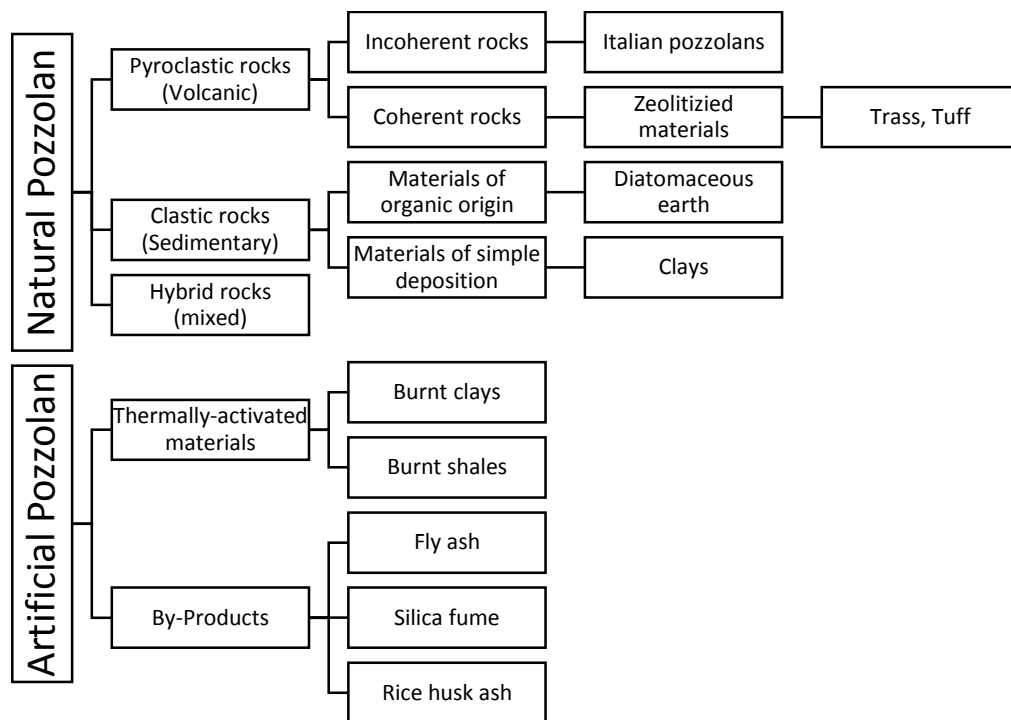


Figure 3.1 Classification of pozzolans (Massazza, 1988)

The common blended cements that are currently in use usually contain natural pozzolans, low-lime fly ashes, GGBFS, and limestone powder. Thus, these four mineral admixtures were used in this investigation. A closer look at them is taken in the subsequent sections.

### **3.1.1. Trass**

Trass which is one of the natural pozzolans of volcanic origin is obtained by the rapid cooling of erupted magma. It is composed mainly of alumina-silicates. Rapid cooling enables magma to have an amorphous structure. Due to reactions among gases taking place during the eruptions, the material gets a porous structure (Ramachandran, 1995).

### **3.1.2. Limestone**

Limestone is primary raw material of cement. Besides, it can be used as a mineral admixture. Although there is no contribution of limestone on compressive strength at later ages when used in small amounts, it may accelerate the hydration of portland cement and thus result in slightly higher strengths at early ages. The primary reason for using limestone in blended cements is related with its beneficial effect on workability (Erdoğan, 2002).

### **3.1.3 Fly Ash**

Thermal power plants burning solid fossil fuels for generation of electricity are used throughout the world. One of the solid fossil fuels is pulverized coal. The burned pulverized coal produces three main waste materials: bottom ash, boiler slag and fly ash which constitutes 75-80% of the waste materials (Özdemir, 2001). The fly ash, which is a waste product of thermal power plants widely produced all over world, is one of the mineral admixtures commonly used in cement and concrete industry due to aforementioned ecological and economical reasons in addition to its beneficial effects on concrete properties. There are several different ways of classifying fly ashes according to their compositions.

Widely known ones are ASTM C618 (2012), EN 197-1 (2012), according to its CaO content (Dhir, 1986) and according to its SiO<sub>2</sub>, Al<sub>2</sub>O<sub>3</sub>, CaO and SO<sub>3</sub> contents (Tokyay and Erdoğdu, 1998). There is no information concerning the origin of fly ash types in classifications proposed by EN 197-1 (2012) and Dhir (1986). Comparison of these 4 general classes of fly ashes according to their chemical compositions is shown in Table 3.1.

Table 3.1 Comprasion of fly ashes classified according to their chemical properties

Chemical Requirements		S+A+F	Reactive S	Reactive C	C	Free C	S+C	$\bar{S}+C$	S+A
ASTM (2012)	Class F	$\geq 70\%$	—	—	—	—	—	—	—
	Class C	$\geq 50\%$	—	—	$>10\%$	—	—	—	—
EN (2012)	V-Type	—	$\geq 25\%$	$\leq 10\%$	—	$\leq 1\%^*$	—	—	—
	W-Type	—	$< 25\%$	$> 10\%$	—	—	—	—	—
Dhir (1986)	Low Lime	—	—	—	$<10\%$	—	—	—	—
	High Lime	—	—	—	$>10\%$	—	—	—	—
Tokyay and Erdoğdu (1998)	Si-Al	—	—	—	—	—	—	—	Higher
	Su-Ca	—	—	—	—	—	—	Higher	—
	Si-Ca	—	—	—	—	—	Higher	—	—

\*Free C content in V-Type Fly Ash is allowed up to 2.5% unless soundness exceeds 10 mm upon testing a mixture with 30% by mass V-Type Fly Ash, and 70% by mass Cement I conforming to EN 197-1.



#### **3.1.4. Blast Furnace Slag (BFS)**

Blast Furnace Slag (BFS) is a by-product of pig iron production. Depending on the cooling process used, there are three types of BFS: Air-cooled, expanded and granulated. Air-cooled BFS due to its crystalline structure and expanded BFS due to its highly porous and partly crystalline structure may not be used as mineral admixtures in concrete. Granulated BFS with its almost completely glassy structure, is suitable in cement and concrete industry as mineral admixture after finely grinding. (Tokyay, 2016)

### **3.2. Influence of Mineral Admixtures on Hydration**

Mineral admixture incorporation affects the hydration process both physically and chemically.

#### **3.2.1. Physical Influence**

The physical effects of mineral admixtures on hydration have four aspects: (1) Cement dilution effect, (2) Dispersion effect, (3) Modification of particle size distribution, and (4) Nucleation effect. The first one is observed when the mineral admixture is used as a partial replacement for portland cement. Decreased amount of portland cement portion results in less hydrated material (Tokyay, 2016).

Portland cement particles have the tendency to coagulate when mixed with water. Incorporation of fine mineral powder into the system leads to the dispersion of the cement particles thus reducing the tendency for flocculation and exposing more cement surface area for hydration (Dhir, 1986). At the same water-solids ratio, the water-portland cement ratio becomes higher and allows more space for hydration of clinker phases (Lothenbach et al., 2011). Furthermore, the dispersion effect leads to a

more homogeneous distribution of water within the cement paste and thus facilitates the hydration. In other words, for a fixed cement amount, mineral admixture incorporation would result in more cement hydration.

Water availability for hydration is enhanced by the clogging of capillary channels in the fresh paste by fine mineral admixture particles. Reduced bleeding upon the prevention of capillary water movement leads to more water being available for hydration. Another physical effect related with modification of particle size distribution by mineral admixtures is the possible reduction in the thickness of initial layer of hydrates formed on the surface of the cement particles. Such a reduction in the thickness of the initial hydrate layer makes breaking it down easier thus accelerating the hydration process.

The presence of mineral admixtures facilitates the early hydration of portland cement also by providing additional sites for the precipitation of hydration products (Lawrence et al., 2003; Dhir, 1986; Halse et al., 1984). It is related with the fineness of the mineral admixture and its affinity for cement hydrates.

All four physical effects discussed above are true for any kind of mineral admixture whether it is non-reactive, pozzolanic or hydraulic. Mineral admixtures enhance the hydration of the portland cement portion of the cementitious system in which they are incorporated. However, this may be suppressed if the amount of mineral admixture used is high. (Tokyay, 2016).

### **3.2.2. Chemical Influence**

Pozzolans and latent hydraulic materials are involved in the hydration process chemically, also. Pozzolanic and/or hydration reactions of the mineral admixtures and their interactions with the hydration of portland cement form the three main parts of their chemical involvement in the hydration process. This chemical involvement depends on their (1) chemical and (2) mineralogical compositions, (3) amount of

glassy phase, (4) fineness, (5) amount, (6) the characteristics of the cement that they are used with, and (7) ambient temperature and humidity. The general term pozzolanic activity refers to all chemical reactions between pozzolans, lime, and water. Generally two parameters are used to describe the activity of any pozzolan: (1) Lime combining capacity and (2) rate of lime combination (Massazza, 1988).

Lime combining capacity of a pozzolan depends on the followings:

1. The nature and amount of the active phases present;
2. The silica content;
3. Relative proportions of lime and pozzolan in the mix;
4. Curing period.

On the other hand, the rate of lime combination by a pozzolan depends on

1. Fineness of pozzolan;
2. Water-solids ratio of the pozzolan-lime-water mixture;
3. Ambient temperature.

GGBFS and high-lime fly ashes can behave as hydraulic binders if they have an appropriate chemical composition. However, these materials usually need suitable activators to exhibit hydraulic reactivity, unlike portland cements which react readily with water, alone. This is why they are called latent hydraulic materials.

Hydration of latent hydraulic materials require either alkaline or sulfatic activators such as  $\text{Ca}(\text{OH})_2$ ,  $\text{NaOH}$ ,  $\text{KOH}$ ,  $\text{Na}_2\text{SiO}_3$ , and calcium sulfates (gypsum, hemihydrate, anhydrite) (Odler, 2000).

Portland cement-GGBFS blends contain both the alkaline and the sulfatic activators. Calcium hydroxide from the hydration of  $\text{C}_3\text{S}$ , sodium and potassium hydroxides that form from the alkalies in the portland cement portion and gypsum which is present in the portland cement as a retarder are the activators for the hydration reactions of GGBFS.



## CHAPTER 4

### REVIEW OF RECENT RESEARCH

The classical work and the background for concrete maturity were considered in Chapter 2. This chapter reviews the recent research work related with maturity of concrete reported in the last fifteen years.

Eren (2002) studied the strength development of GGBFS or fly ash-incorporated concretes subjected to different curing temperatures (6, 20, 35, 60, 80°C) and compared the results with those of the control concretes. Five types of mixes used were ordinary portland cement, 30% and 50% of supplementary cementitious (by mass of total cementitious material). A function, proposed by Carino, given in Equation (2.9) was used in the study to establish compressive strength-ages relationships.

To achieve better fits at high temperatures (40-60°C), a power index,  $n$ , which depends on temperature, introduced by Brooks and Al-Kaisi (1990) was included in Equation (2.9) to obtain the following relationship:

$$S = S_u \cdot \frac{k_T \cdot (t - t_0)^n}{1 + k_T \cdot (t - t_0)^n} \quad (4.1)$$

When considering the results, the following conclusions were deduced:

- Ordinary portland cement showed higher compressive strength than the one of pozzolanic portland cements at all temperatures except for 35°C which is the most appropriate temperature gives higher compressive strength for fly ash-incorporated concretes.

- Equation (4.1) describes strength-age relationship more correctly than Equation (2.9).

Kasap (2002) investigated the effects of 4 different types of cements (i.e. ordinary portland cement, portland composite cement, sulfate-resisting portland cement and blast furnace slag cement) on concrete maturity by relating it to the heat of hydration of the cement used. The validity of some maturity functions in the study was also analyzed, and they proposed an easy way to calculate equivalent age by  $E_a$  derived from the degree of hydration and the rate of hydration relationships:

$$E = R \left( \frac{T_1 \cdot T_2}{T_1 - T_2} \right) \left[ \ln \left[ (1 - a) \frac{K(T_1)}{K(T_2)} \right] \right] \quad (4.2)$$

where,

$E$  : Apparent activation energy

$R$  : Gas constant, [8.314 J/mol-°K]

$T_1$  and  $T_2$  : Temperature [°K],

$a$  : Amount of admixture,

$K$  : A kinetic constant related to the hydration of concrete.

The kinetic constant is a coefficient in the rate of hydration-degree of hydration exponential curve. The constant depends on curing temperature and mixture type, so it should be calculated for each temperature and for each mixture.

Besides, they showed the applicability of common maturity functions for 4 different types of cements.

Barnett et al. (2006) followed up an experimental study concerning investigation of strength developments and establishment of  $E_a$  of mortars containing GGBFS (0, 20, 35, 50 and 70 % replacements which were made on an equal mass basis) under the

different curing temperature (i.e. 10, 20, 30, 40 and 50°C). In the study, choice of GGBFS as pozzolan is due to its drawbacks related to common use areas such as mass concrete where heat propagation takes a long time and that its slower strength improvement under the room temperature.

$E_a$ , calculated by means of Arrhenius equation, of 0, 20, 35, 50 and 70 % GGBFS as replacement by mass for cement were approximately 34, 36, 50, 52 and 60 kJ/mol, respectively. The conclusions from the paper are listed below:

- It can be easily inferred from the graphs upon comparing to portland cement, mortars with GGBFS have higher compressive strength at early ages, especially at higher temperatures due to having greater rate of reaction. At later ages, however, the situation is completely reversed, that is, GGBFS mortars have lower strength owing to the formation of the dense hydrated particles placed around the cement particles as unreacted.

Abdel-Jawad (2006) proposed an equation for the estimation of compressive strength of concrete at later ages. The method included basically the effect of w/c in Nurse-Saul equivalent age function and considered the effect of different constant curing temperatures on compressive strength of concrete at later ages. This relationship is given by following equation:

$$\frac{f_c(t, T_a)}{f_c(t_e, T_s)} = 1 - k \frac{T_a - T_s}{T_s} \quad (4.3)$$

where,

$f_c(t, T_a)$  : Strength at time  $t$ , and average concrete temperature  $T_a$ ,

$f_c(t_e, T_s)$ : Strength at equivalent age  $t_e$ , and specified temperature  $T_s$ ,

$k$  : A factor depending on  $t_e$ .

The relationship between  $k$  and  $t_e$  is given by following equation,

$$k = 0.14 \cdot (1 - e^{-0.1t_e}) \quad (4.4)$$

Equation (4.5) to predict compressive strength of concrete at later ages was derived from Equation (4.3) and Equation (4.4):

$$f_c(t, T_a) = f_c(t_e, T_s) \cdot \left[ 1 - 0.14 \cdot \left( \frac{T_a - T_s}{T_s} \right) \cdot (1 - e^{-0.1t_e}) \right] \quad (4.5)$$

Following conclusions were drawn:

- The proposed model gives results with low margin of error in the mortars prepared with Type I portland cement, and should be examined under the different conditions as variable temperatures and/or mortars with different type of cements and/or chemical and mineral admixtures.

Voigt et al. (2006) examined the relationship of two the non-destructive methods (NDT), the maturity method and ultrasonic wave reflection (WR) method, on the cement mortars having different water/cement ratios and cured at the different temperatures. WR-method is based on the basis of monitoring the reflection loss of shear waves at surface between a plate and mortars. The loss of shear waves depends on the reflection coefficient, and state of the tested mortar. Thus, degree of hydration has a vital significance on the transmission of shear waves. On the other hand, the maturity method is mainly based upon roughly calculating early-age compressive strength of concrete. One of the major deficiencies concerning the maturity is not to calculate some concrete properties, but WR-method gives information about setting time, capillary porosity, and extent of hydration besides compressive strength of the mortar. This makes it more outstanding or preferable.

The following observations are drawn for the mortars:



- There is no significant effect of water/cement ratio, composition of the mortar or curing temperature on reflection loss-strength relationship. Water-cement ratio, however, have especially important to establish equivalent age-compressive strength curve.
- WR-method gives more accurate results compared with that of maturity method, especially beyond 36 h. The reason is owing to heterogeneity of the concrete microstructure.

Zhang et al. (2008) discussed capabilities and restrictions of the maturity method and proposed a new approach for high performance concretes (HPC). Main restrictions about available maturity method are (a) decision of essential formula for calculation of maturity index necessary for determination of activation energy,  $E_a$  and (b) establishment of relationship between the strength and maturity index. The paper was mostly concentrated on strength data during the first 7-day of the hydration. In order that, the accuracy of analyses (i.e. compressive strength-maturity, compressive strength-time after setting, tensile strength-time after setting, degree of hydration-time after setting, modulus of elasticity-time after setting, activation energy-compressive strength, activation energy-tensile strength, activation energy-degree of hydration, tensile strength-maturity, modulus of elasticity-degree of hydration) is increased. However, strength results at 28-day are available in the paper as additional information. The paper adopted an idea of using an activation energy range for the mixture in contrast to the idea of specifying a single activation energy value for the mixture. The approach was implied as “Slope Method”. The method considered different temperature ranges: (10-25°C, 25-40°C, and 10-25-40°C) to determine activation energy of HPC. Besides, the paper examined relationships between activation energy and compressive strength, Young’s modulus, tensile strength, and degree of hydration by using Slope Method, Arrhenius equivalent age function and Equation (2.9). The following conclusions and recommendation were drawn in the paper:

- Equation (2.9) gives more accurate results than the other methods for all analysed properties of HPC.
- The proposed method should be checked for other concrete types.

Vázquez-Herrero et al. (2012) carried out a study for the examination of a new procedure concerning the structural safety, established on the maturity method, as a non-destructive test method used for estimation of compressive strength of in-place concrete, and limit state theory. The theory basically asserts that a structure is as satisfying as its weakest member. For this purpose, the maturity method was mainly employed to check the compatibility of previous studies and to decide on the earliest possible stripping time of formwork in false tunnels at early-ages. In order to carry out the research, temperature sensors were embedded in both north side-wall and south side-wall of the member to plot temperature-elapsed time since casting, necessary for applicability of maturity method. The safety coefficient,  $\gamma_t$ , another aim of the study, was applied for calculation of the earliest possible time of formwork removal.

Based on the results, the conclusions arrived are listed below:

- Embedding of sensors to the two different sides enabled assessment of structure in terms of the safety owing to occurrence of two different extreme temperatures.
- $\gamma_t$  is beneficial to the worker and structure since the time for formwork removal is larger than that obtained from equivalent age-elapsed time since casting graph, a conventional method used in maturity.
- Equivalent activation energy in the proposed procedure is a variable parameter, and the necessity to specify its limits experimentally is absolutely crucial with regard to safety.

Boubekeur et al. (2014) conducted an experimental study on the estimation of compressive strength of two groups of mortars made with three mineral admixtures at different curing temperature by maturity method. Mineral admixtures used in this study were limestone powder (10% by mass), natural pozzolan (20% by mass) and

blast furnace slag (30% by mass) for both groups. In the first part of experiment, mortars were subjected to constant temperatures of 20, 30, 40 and 50 °C for 1, 3, 7, 28, 90-day. In the second part of experiment, mortars were exposed to variable temperatures of 30, 40 and 50 °C for 1, 3, 7, and 28-day. When they were taken out from curing pool at initial curing temperature, curing process continued at 20 °C until the test day. It was concluded that:

- The increase in compressive strength was linearly proportional to the increase in temperature, at early ages, for all mortars.
- Mortars with natural pozzolan and blast furnace slag had higher compressive strength than those of ordinary portland cement and limestone incorporated mortars at later ages. Main reason of that is pozzolanicity of natural pozzolan and latent hydraulicity of blast-furnace slag. On the other hand, the temperature rise led to decreasing compressive strength of all mortars at later age when compared to 20°C curing temperature.
- Maturity method does not give accurate results above 350°C·day. This is due to nonlinear relation between the maturity and the strength.
- The compressive strength at later ages can be estimated by equivalent maturity, but the limitation maturity value, 350°C·day, should not be ignored.

Yikici and Chen (2015) performed a study to predict in-place strength of four cube concrete members of 1.8 m side. Therefore, 150 x 300 mm cylinder samples were taken from construction site to establish strength-maturity relationship. After that, temperature sensors were embedded into different points of the cube concrete members. Also, four core specimens with 10 cm diameter were collected from different points of mass concrete at 4, 28 and 56-day. Then, estimated strength by 150 by 300 mm samples and measured strength by core specimens were compared and following conclusions were attained based on the results:

- Core compressive strength depended on location of the cube block. Predicted strength using maturity method was higher than core strength on the top portion, and it was within 15% of the core results at the center of cubes, but it was lower than core drilled from bottom surface.
- The temperature was highest at middle section, and it also depended on the location of the cubes.

Lee and Hover (2015) carried out a study associated with the effect of  $T_0$  and  $E_a$  on strength estimation by maturity method. For this purpose, 4 different sets data from an earlier work (2 set data) and author's own data (2 set data) were examined to create an iterative method based on increment of factuality of results by altering inputs constantly until reaching minimum margin of error for the results. Following results were obtained by analyzing the results of the study:

- The selection of appropriate values of  $T_0$  and  $E_a$  significantly affected the relationship between maturity and compressive strength.
- It is advisable to use default values of  $T_0$  and  $E_a$  within the ASTM C1074 for the simple-ordinary mixtures, but making a modification of  $T_0$  and  $E_a$  values for other or complex mixtures is a crucial matter so as to confront with minimal errors.
- The iterative method generally defines the values of  $T_0$  and  $E_a$  with minimum possible error.

Ferreira et al. (2015) studied on characterization of alkali-activated mortars and concretes employing maturity method. Only fly ash as an alkali-activated binder, four different alkaline solutions, only NaOH with 8 M and 12 M, mixture of 60% NaOH with 12 M and 40% sodium silicate solution and mixture of 40% NaOH with 12 M and 60% sodium silicate solution, and replacement 10% of binder by portland cement were used in the study. According to results obtained by 8 different mixtures to be used Nurse-Saul and Arrhenius equations;

- Calculated  $T_0$  and  $E_a$  values are compatible with experimental results except for mixture (100% fly ash) containing NaOH with 12 M and the mixture (90% fly ash + 10% portland cement by weight) containing NaOH with 8 M.

- The strength of the mixtures can be estimated with lower than 20% error.
- Arrhenius equation incorrectly evaluates the compressive strength of the mixtures for early ages.



## **CHAPTER 5**

### **5. EXPERIMENTAL PROGRAM**

This chapter provides the details of mixture proportions, materials used, and some tests for materials.

#### **5.1. Materials**

##### **5.1.1. Cement and Mineral Admixtures**

The portland cement (CEM I 42.5), trass and limestone used in the study were supplied by ÇimSA, and fly ash was obtained from Tunçbilek Thermal Power Plant.

Their chemical compositions, Blaine fineness values and densities are given in Table 5.1. The chemical analyses were carried out in the R&D Laboratory of TCMA.

Table 5.1 Chemical and physical properties of materials used

Properties (%)	Limestone	Fly Ash	Trass	GGBFS	PC
SiO <sub>2</sub>	1.40	53.20	69.74	42.96	18.62
Al <sub>2</sub> O <sub>3</sub>	0.09	22.89	12.02	11.28	4.94
Fe <sub>2</sub> O <sub>3</sub>	0.08	6.15	1.74	0.87	2.46
CaO	52.18	6.28	2.82	33.01	61.61
MgO	2.80	2.22	0.86	6.16	2.27
SO <sub>3</sub>	0.04	1.15	0.05	1.45	3.29
Na <sub>2</sub> O	0.06	0.92	1.10	0.33	0.32
K <sub>2</sub> O	0.09	1.41	1.78	0.66	0.80
TiO <sub>2</sub>	—	1.09	0.33	0.60	—
Cl <sup>-</sup>	—	—	—	—	0.0091
LOI	43.10	2.98	7.27	0.33	5.12
Fineness [cm <sup>2</sup> /g]	5200	4500	5400	4700	3400
Density [g/cm <sup>3</sup> ]	2.72	2.42	2.28	2.90	3.04

### 5.1.2. Standard Sand

CEN standard sand was obtained from Limak Batı Çimento San. ve Tic. A.Ş.

### 5.1.3. Water

Quality of water used for mixing has an important role on the all mortar properties like compressive strength. Tap water was used throughout the study.

### 5.1.4. Mixture Proportions

Thirteen different mortar mixtures were used in the study. The Control mixture was prepared from portland cement. Mineral admixture-incorporated specimens were



prepared by using trass, limestone, fly ash, and GGBFS to replace 6, 20 and 35% (by mass) of the portland cement. The water contents of the mixtures were adjusted such that the flow of the fresh mortar will be  $110 \pm 5$  %. The designation and material properties of the mortar mixtures are given Table 5.2.

Table 5.2 Mortar mix proportions

Group Name	Cement [g]	Mineral admixture [g]	Sand [g]	Water [g]	(w/c)
Control	450	-	1350	252.0	0.56
T-6	423	27	1350	265.5	0.59
T-20	360	90	1350	301.5	0.67
T-35	292	158	1350	319.5	0.71
LS-6	423	27	1350	252.0	0.56
LS-20	360	90	1350	252.0	0.56
LS-35	292	158	1350	252.0	0.56
FA-6	423	27	1350	252.0	0.56
FA-20	360	90	1350	252.0	0.56
FA-35	292	158	1350	234.0	0.52
S-6	423	27	1350	252.0	0.56
S-20	360	90	1350	252.0	0.56
S-35	292	158	1350	252.0	0.56

## 5.2. Test Methods

### 5.2.1. Tests on Pastes

#### 5.2.1.1. Normal Consistency and Setting Time Tests

The normal consistency test was applied on pastes having a mixing procedure in accordance with ASTM C 305 standard, as compatible with ASTM C 187 standard. After water-cementitious (w/c) ratios for normal consistency were decided, setting time tests were done according to ASTM C 191 standard.

## **5.2.2. Tests on Mortars**

### **5.2.2.1. Mixing and Moulding Procedure**

Manual mortar mixer, three-gang [40x40x160 mm] molds, and jolting apparatus were used. Mixing, moulding and compaction procedures of all mixtures were done in accordance with EN 196-1 standard.

### **5.2.2.2. Flow Test**

Flow test was carried out according to ASTM C 1437 standard. Compaction process is affected by properties of ingredients (fineness, surface texture, roughness, etc.), water content in mixture have a significant impact on properties of fresh and hardened mortars. To avoid this unstable factor, mixtures having  $110 \pm 5$  % flow capacity were used all through the study instead of mixtures having a constant w/c.

### **5.2.2.3. Compressive Strength**

The standard compressive strength test method of EN 196-1 was applied on mortar specimens at 2 d, 7 d, 14 d, 28 d and 90 d. Three batches of cement mortar consisted of 3 prismatic specimens of 40 mm x 40 mm x 160 mm for each group were tested for the specified age. Compressive strength were the average of six broken pieces obtained after flexural testing.

### **5.3. Curing Conditions**

As specified by ASTM C 1074, three different curing conditions are required for determination of  $T_0$ . Thus, prism specimens of 40 mm x 40 mm x 160 mm were cured isothermally at 5°C, 20°C and 40°C.



## CHAPTER 6

### 6.1 DISCUSSION AND RESULTS

The compressive strength test results for all mixtures are given in Table 6.1.

Table 6.1 Compressive strength test results

Mixture	Age [days]	Compressive Strength [MPa]		
		5°C	20°C	40°C
Control	2	14.13	20.82	28.42
	7	24.47	33.02	41.02
	14	32.53	40.90	46.87
	28	38.35	46.95	49.93
	90	48.27	52.15	50.42
T-6	2	9.07	12.33	18.62
	7	19.35	27.83	39.47
	14	27.45	36.22	44.50
	28	34.50	40.73	44.75
	90	40.43	45.22	45.17
T-20	2	6.20	9.30	14.00
	7	13.9	19.30	27.00
	14	18.00	25.50	32.00
	28	23.8	32.00	36.00
	90	31.4	39.9	35.70
T-35	2	2.90	4.98	7.00
	7	8.18	11.08	19.10
	14	9.62	16.45	22.50
	28	12.54	20.87	26.93
	90	17.55	27.82	28.00

Table 6.1 (continued)

LS-6	2	11.08	18.90	21.52
	7	20.47	26.18	35.95
	14	30.23	38.63	43.33
	28	38.67	40.68	44.68
	90	47.33	47.92	46.48
LS-20	2	11.20	14.63	18.38
	7	20.60	27.37	31.73
	14	24.82	33.58	35.97
	28	31.11	39.44	40.37
	90	35.57	41.15	40.08
LS-35	2	6.80	11.60	13.50
	7	15.10	21.50	22.60
	14	19.00	24.70	24.00
	28	22.50	28.60	27.40
	90	28.30	33.40	27.70
FA-6	2	5.37	10.68	20.82
	7	21.33	32.67	39.03
	14	27.47	41.77	50.25
	28	33.90	45.25	52.80
	90	47.03	54.72	59.28
FA-20	2	4.98	8.72	17.63
	7	16.68	27.03	36.82
	14	24.03	34.42	49.73
	28	27.58	38.92	59.08
	90	35.25	52.48	61.47
FA-35	2	4.95	7.97	14.25
	7	14.78	22.72	35.43
	14	20.22	28.4	48.53
	28	24.05	35.72	55.27
	90	31.57	51.82	60.92
S-6	2	13.43	19.00	25.15
	7	22.90	25.07	36.92
	14	29.87	39.63	44.62
	28	39.30	46.13	47.57
	90	51.47	57.37	52.58
S-20	2	10.27	14.63	21.02
	7	16.80	23.52	33.93
	14	20.97	27.77	39.82
	28	28.23	44.50	57.48
	90	38.20	54.75	58.92
S-35	2	6.90	10.80	16.30
	7	12.90	19.20	35.00
	14	21.60	30.20	44.10
	28	24.00	40.60	51.40
	90	34.60	48.30	54.58

It was expected that the strength would increase as the temperature was increased owing to accelerating hydration reactions and pozzolanic reactions. This expectation was generally obtained in a large majority of the mixtures.

It could be found that some mixtures did not obey this rule. Especially, the strength of the some mixtures such as LS-20 and LS-35, with higher amounts of mineral admixture decreased even the temperature was increased. This behavior may be due to dilution effect. Upon increasing the amount of mineral admixtures increases, cement content in the mixture decreases. This leads to less hydrated cement which causes less compounds with binding value. Besides, another exception emerged in some mixtures such as Control at 40°C, T-20 at 40°C, S-6 at 40°C. The reason may be due to cross-over effect. As stated by Malhotra and Carino (2004), under high temperatures, fast formed hydration products may cause a considerable porosity in the matrix. This brings about loss of ultimate strength in the mixtures. This phenomenon is known as the cross-over effect.

### **6.1. Analysis of Data Based on ASTM C1074 Methods**

ASTM C1074 (2011) offers three different options (A1.1.7, A1.1.8.1, and A1.1.8.2) to determine  $T_0$  and  $E_a$  as already stated in Chapter 2.3. The procedures and the calculations of  $T_0$  and  $E_a$  for each options are explained by an example in Appendix A. As can be seen from Appendix A, major similarity for these options is that the same steps (i.e. determining  $T_0$  and  $E_a$ ) are followed after determining of k-values. By considering this fact, temperature sensitivity values utilizing the three options for each type of mixture are summarized in Table 6.2.

Table 6.2  $T_0$  and  $E_a$  values according to the proposed approach

Mixtures	A1.1.7		A1.1.8.1		A1.1.8.2	
	$T_0$ , [°C]	$E_a$ , [J/mol]	$T_0$ , [°C]	$E_a$ , [J/mol]	$T_0$ , [°C]	$E_a$ , [J/mol]
Control	-15.86	19283	-6.95	24686	1.61	37923
LS-6	-33.08	15965	-4.04	32632	0.77	33402
LS-20	-51.98	9329	-0.60	39019	-2.00	30810
LS-35	-14.77	20924	0.80	37191	5.07	45432
T-6	-26.57	14364	-15.94	21222	4.91	45325
T-20	-24.56	15214	-7.52	34240	4.06	39682
T-35	-104.91	5806	-3.88	34220	-0.46	31000
FA-6	1.00	38183	-0.89	25667	-75.81	7334
FA-20	-8.68	23412	-4.51	25510	-34.83	11995
FA-35	-48.81	10264	-3.27	26881	-23.66	14658
S-6	-24.78	15795	-6.91	26565	-27.77	15537
S-20	-154.65	3924	-10.22	23629	-0.51	26108
S-35	-122.69	5046	-1.38	26921	-0.07	32749

The idea behind determination of  $T_0$  for Option A1.1.7 is selection of an acceptable point (say rate constant) which is valid for all ages and all temperatures to which concrete is exposed. Similar logic can be expressed for determination of  $E_a$ . Thus, choice of temperature to which concrete may be exposed, has a significant effect on determination of  $T_0$  and  $E_a$ . Besides, the option may not give the correct result in mineral admixture-incorporated mortars at early and late ages because deviations among points used for a straight line in the reciprocal of strength vs. reciprocal of age beyond time of final setting time graphs prevent correct determination of  $T_0$  and  $E_a$  of these mortars. This is thought to be caused by the effect of mineral admixtures on hydration.



Among these three methods, only A1.1.7 requires the final setting times of the mixtures to determine k-values. Thus, final setting times together with initial setting times at 20°C and w/c required to normal consistency for each mixture are given in Table 6.3.

Table 6.3 Initial - final setting times 20°C and w/c required to normal consistency for each mixtures

Mixtures	w/c	Initial Setting Time [min]	Final Setting Time [min]
Control	0.287	170	300
T-6	0.290	155	300
T-20	0.312	165	360
T-35	0.340	190	420
LS-6	0.277	160	300
LS-20	0.268	150	300
LS-35	0.255	170	310
FA-6	0.275	150	300
FA-20	0.265	170	320
FA-35	0.262	190	350
S-6	0.272	160	305
S-20	0.265	150	285
S-35	0.260	170	295

From Table 6.3, it is obvious that water requirement for pastes with trass is greater than those of limestone, fly ash, or GGBFS even though all of mineral admixtures have similar Blaine fineness values. If water requirement for each type of mineral admixture is compared to that of portland cement separately, as replacement level of trass increases, water requirement is increased. This may be due to irregular shapes of its particles. Water demand of paste with GGBFS for normal consistency is reduced even if the replacement level is increased. The reason is hard and smooth surfaces of its particles which provide lower absorption capacity. Water content of fly ash required for normal consistency is reduced as the replacement level increases.

The reason may be the void filling effect due to its spherical particle shape and finer fraction content. There is no common consensus in the literature whether limestone tends to increase or reduce water requirement of paste, but it was observed in this research that water requirement decreases when its replacement level increases.

In terms of setting time, the results declared that the mineral admixtures, no matter what type of mineral admixture is used, generally increase setting time. The extension of setting time may be due to using lower cement content. As the replacement level of mineral admixtures with portland cement in the mixture increases, it is expected that setting time is extended. Contrarily, GGBFS-incorporated pastes showed shortened setting time. This may be explained by the reaction between GGBFS and water. As a result of this reaction, a thin layer which consists of various chemical components such as silica-rich calcium silicate occurs on the surface of GGBFS's particles. This layer prevents GGBFS's reaction with water, so an activator is needed to continue its hydration reaction (Regourd et al., 1983; Odler, 2000). Since an activator was not used throughout the study, the setting time was extended as its replacement level decreased.

After examining of Option A1.1.7, it can be said for the other two options that they have approximately similar approaches. The origin of both is based on Bernhardt (1956). The study basically explained that strength rate  $d(S)/d(t)$  is a function of the strength and temperature  $T$ , and Bernhardt proposed Equation (6.1) based on empirical results,

$$f(S) = S_u \cdot \left[1 - \left(\frac{S}{S_u}\right)\right]^2 \quad (6.1)$$

where

$f(S)$  : Function of strength,

$S_u$  : Limiting strength at infinite age,

$S$  : Strength at any age,

As explained in 1984 by Carino, upon integrating strength rate and strength functions,

$$\int_0^S \frac{dS}{S_u \cdot \left[1 - \left(\frac{S}{S_u}\right)\right]^2} = \int_{t_0}^t k(T)dt \quad (6.2)$$

If the substitution is used as  $u = 1 - S/S_u$  and  $u' = -S_u \cdot dS$  and the limits of integration is changed as  $u(0) = 1$  and  $u(S) = u$ , the integral becomes,

$$\int_1^u \frac{-du \cdot S_u}{S_u \cdot u^2} = \int_{t_0}^t k(T)dt \quad (6.3)$$

$$\frac{1}{u} + c \Big|_1^u = k \cdot (t) \Big|_{t_0}^t \quad (6.4)$$

$$\frac{1}{u} - 1 = k \cdot (t) - k \cdot (t_0) \quad (6.5)$$

$$\frac{1}{\left(1 - \frac{S}{S_u}\right)} - 1 = k \cdot (t - t_0) \quad (6.6)$$

After re-arranging Equation (6.6), Equation (2.9) can easily be obtained. In fact, Equation (2.9) used in Option A1.1.8.1. and the procedure used in Option A1.1.8.2. have similar approaches. However, there is one difference between them. Option A1.1.8.1 considers the effect of acceleratory period which is age to begin strength development. The period was presented in Equation (2.9) as  $t_0$ . As amount of mineral admixtures in the mortars increases, age to begin strength will be extended. Therefore, there is a paramount significance of this period on determination of  $T_0$  and  $E_a$  for mineral admixture-incorporated mortars. Thus, it is thought that the most appropriate method among the ASTM C1074 for mortars with additives is Option A1.1.8.1.

## 6.2. Strength Development and Nurse-Saul Maturity Function

As stated in ASTM C1074, one of the major limitations of the maturity method is the need to be supplemented by a guide strength development curve. This means that there is a unique strength development each mixture to be used for maturity functions. Therefore, strength-maturity relationship for mixtures should be correctly determined. For this purpose, it is required to determine ultimate strength and the age of the start of strength development in addition to determination of rate constant for each type of mixtures at three temperatures. Equation (2.9) considers the effect of temperature on ultimate strength, age at start of strength development and rate constant. Thus,  $T_0$  attained from option A1.1.8.1. is adopted for maturity functions.

Even though the Nurse-Saul maturity function has some deficiencies as specified in Chapter 2, the function is applied to each type of mixtures separately, and the experimental strength development plots, and experimental strength vs. maturity plots for all mixtures are shown in Figure 6.1 through Figure 6.13 Besides, coefficient of determination of experimental strength vs. maturity for the mixtures are shown in Table 6.4.

Table 6.4 Coefficients of determination of experimental strength vs. maturity for each type of mixture

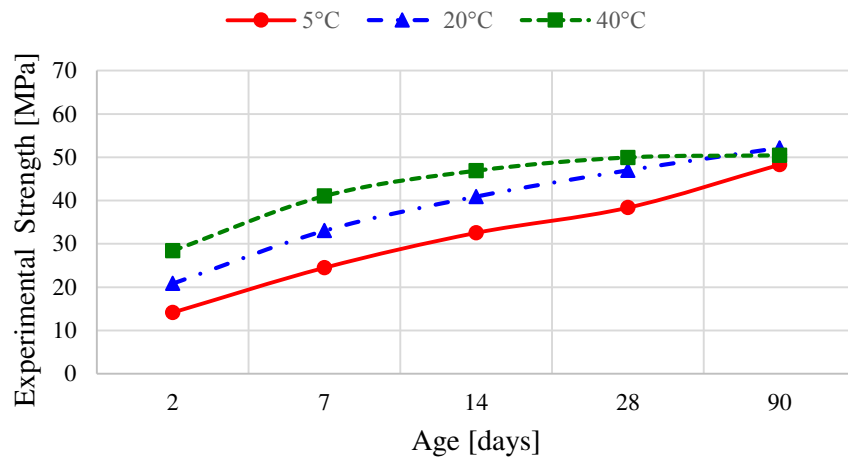
Mixtures	Coefficient of determination
Control	0.93
LS-6	0.92
LS-20	0.92
LS-35	0.89
T-6	0.89
T-20	0.93
T-35	0.93
FA-6	0.96
FA-20	0.94
FA-35	0.91
S-6	0.94
S-20	0.93
S-35	0.94

Regression coefficient enables a great opportunity for interpretation of the results statistically. It can be seen from Table 6.4 that LS-35 has the lowest regression coefficient value. This means that the method will produce higher error for LS-35 than the other mixtures upon using strength-maturity relationship. Similarly, another mixture type having lower regression coefficient value is T-6. It is thought that error may be higher again upon using analogy between strength and maturity.

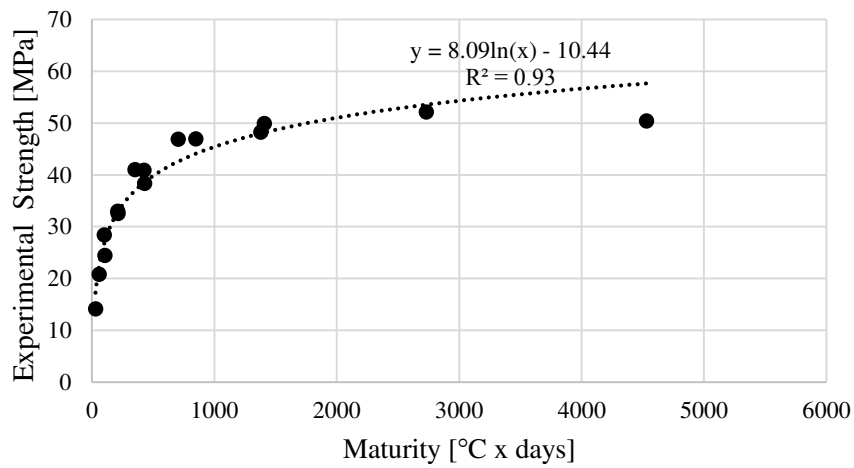
The validity of Equation (2.9) was analyzed and the strengths obtained with the function were compared with experimental strength for each type of mixtures, and the results are presented in Figures B1 to B3 in Appendix B. Besides, the slope values of experimental strength vs. predicted strength for each type of mixtures are shown in Table 6.5.

Table 6.5 Slope values of experimental strength vs. predicted strength for each type of mixtures

Mixtures	Slope
Control	0.81
LS-6	0.83
LS-20	0.87
LS-35	0.96
T-6	0.94
T-20	0.96
T-35	0.96
FA-6	0.95
FA-20	0.95
FA-35	0.95
S-6	0.83
S-20	0.85
S-35	0.98

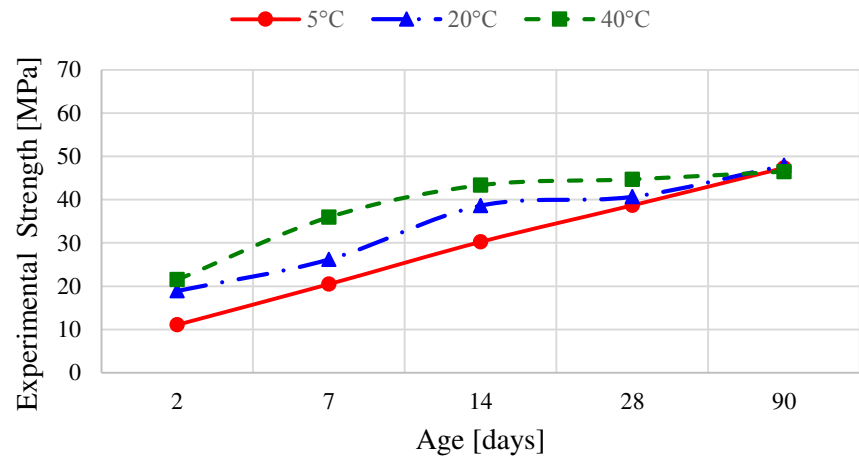


(a)

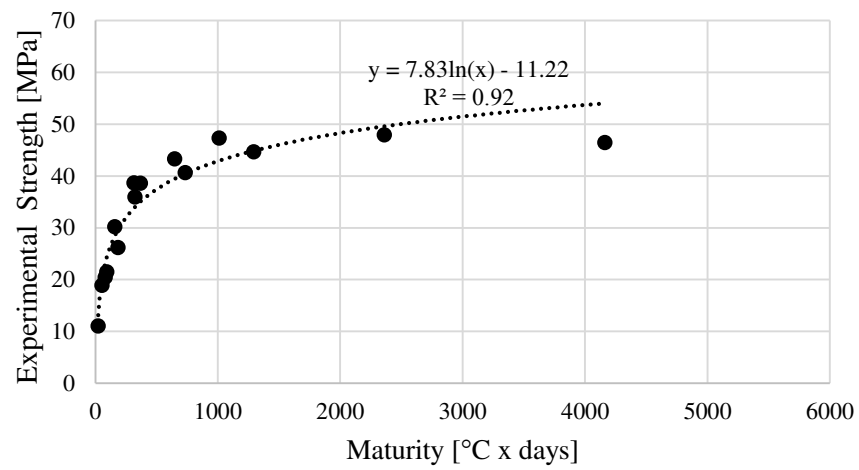


(b)

Figure 6.1 (a) Experimental strength-age (b) Experimental strength-maturity relationships for Control specimens

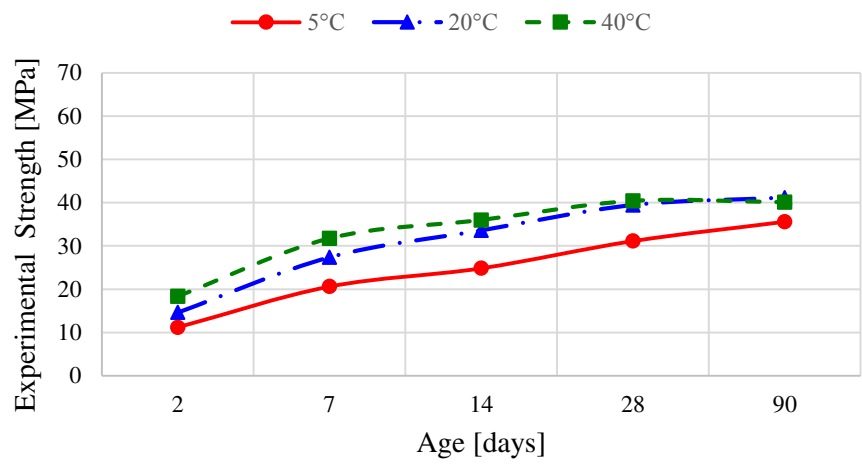


(a)

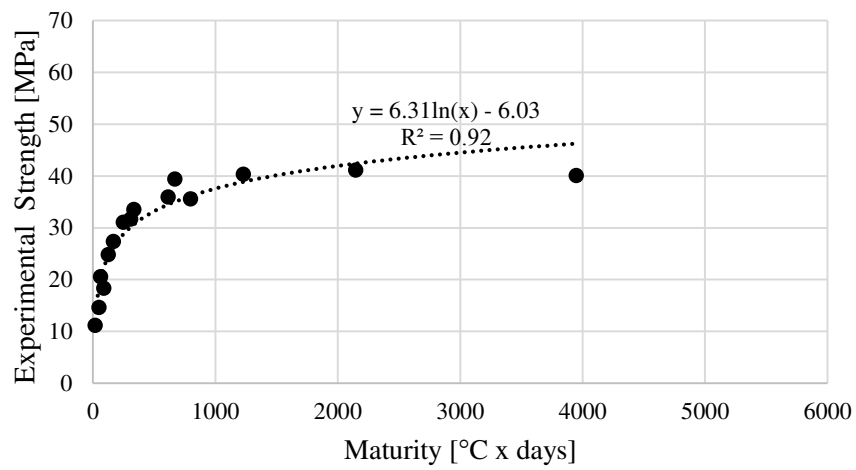


(b)

Figure 6.2 (a) Experimental strength-age (b) Experimental strength-maturity relationships for LS-6 specimens



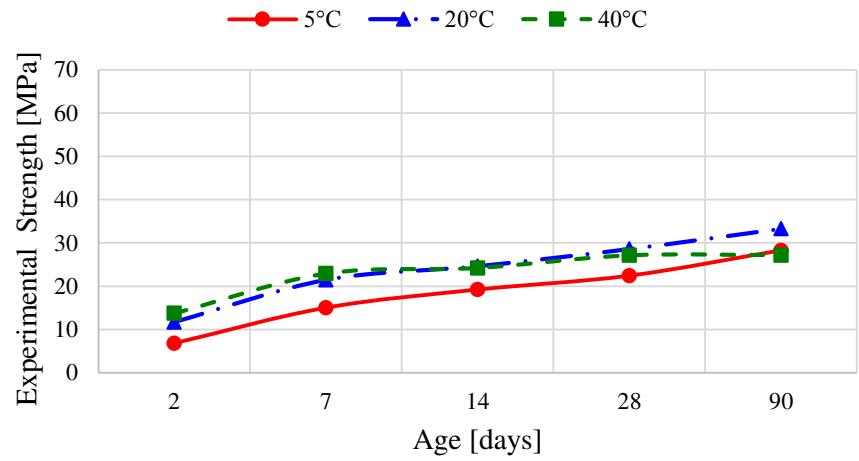
(a)



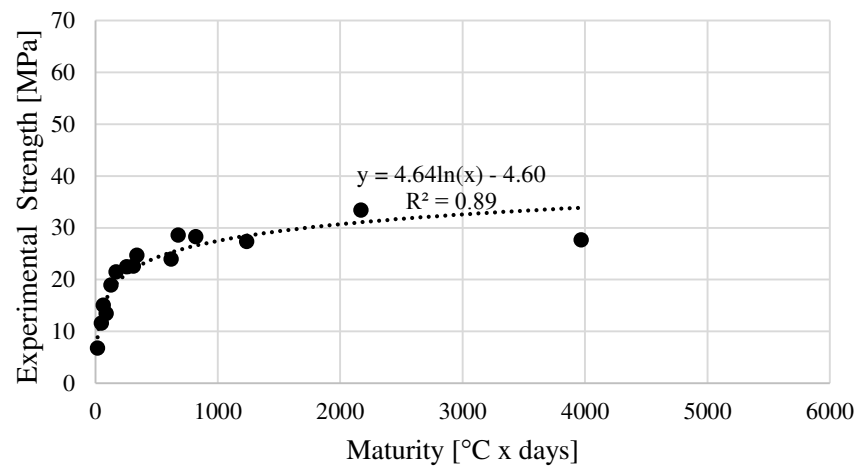
(b)

Figure 6.3 (a) Experimental strength-age (b) Experimental strength-maturity relationships for LS-20 specimens



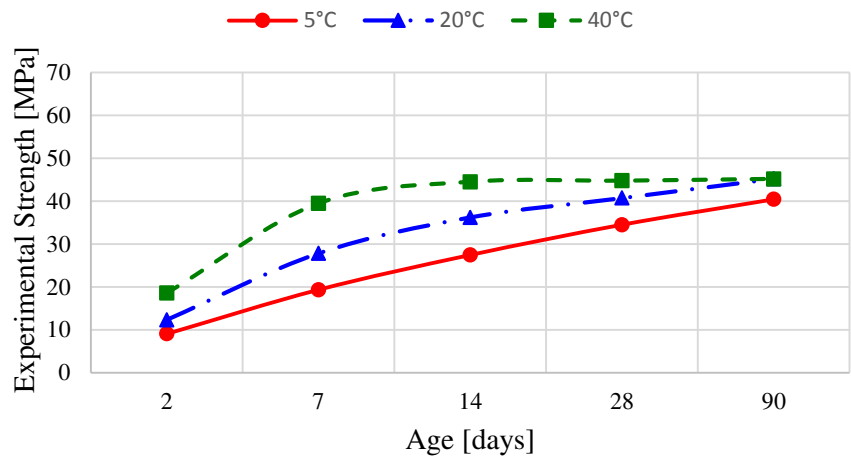


(a)

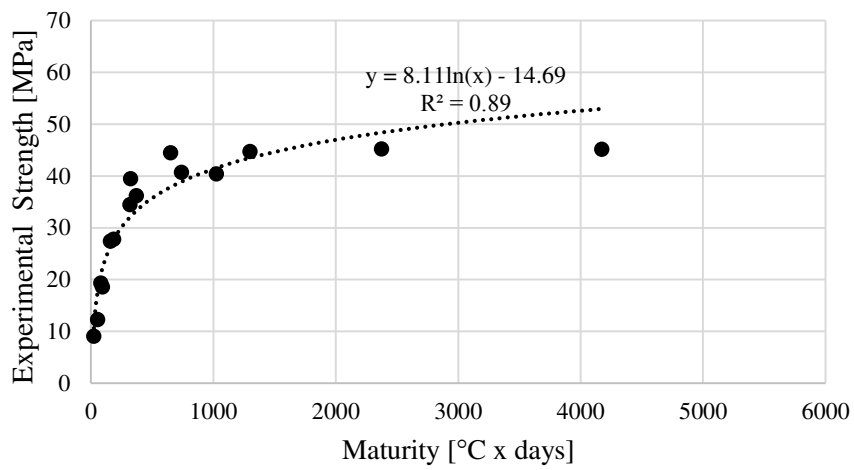


(b)

Figure 6.4 (a) Experimental strength-age (b) Experimental strength-maturity relationships for LS-35 specimens

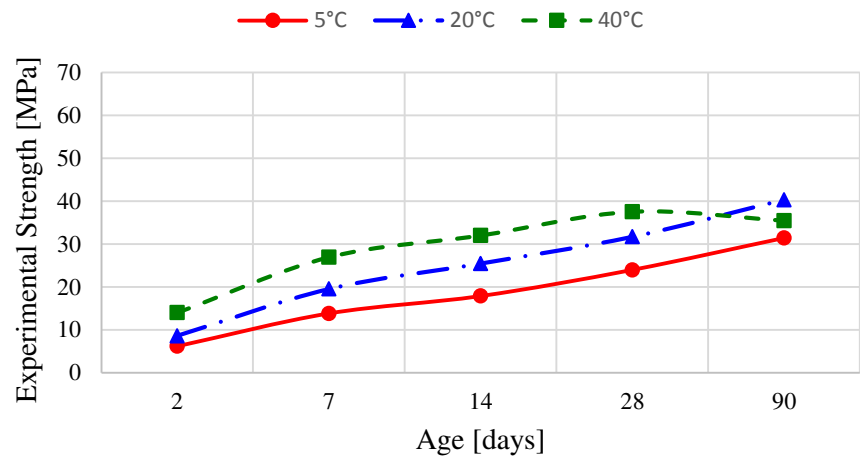


(a)

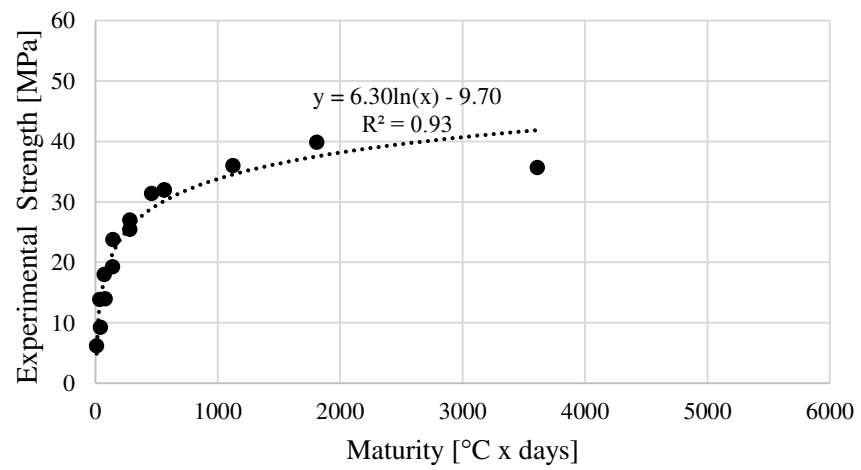


(b)

Figure 6.5 (a) Experimental strength-age (b) Experimental strength-maturity relationships for T-6 specimens

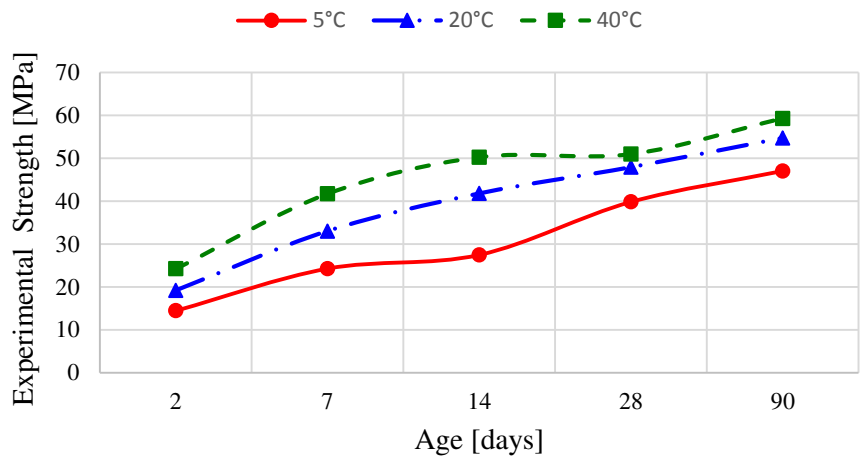


(a)

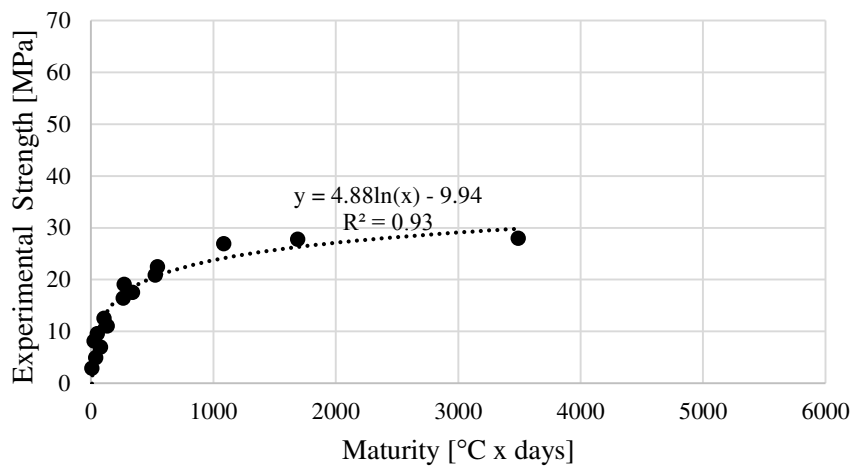


(b)

Figure 6.6 (a) Experimental strength-age (b) Experimental strength-maturity relationships for T-20 specimens

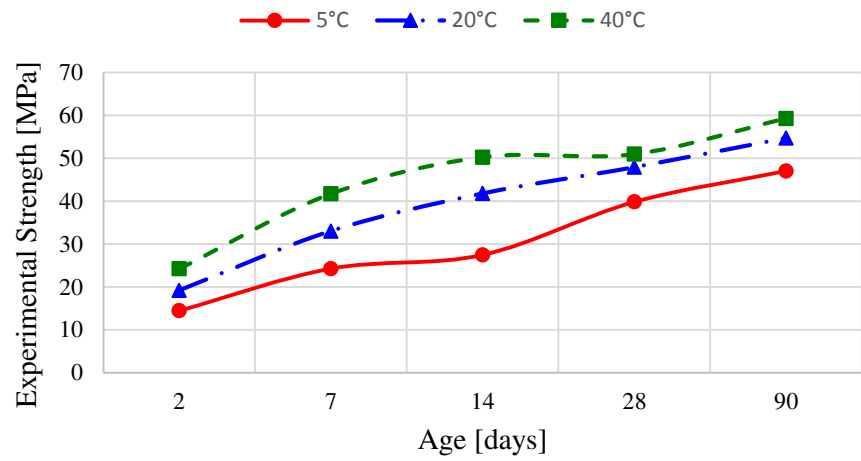


(a)

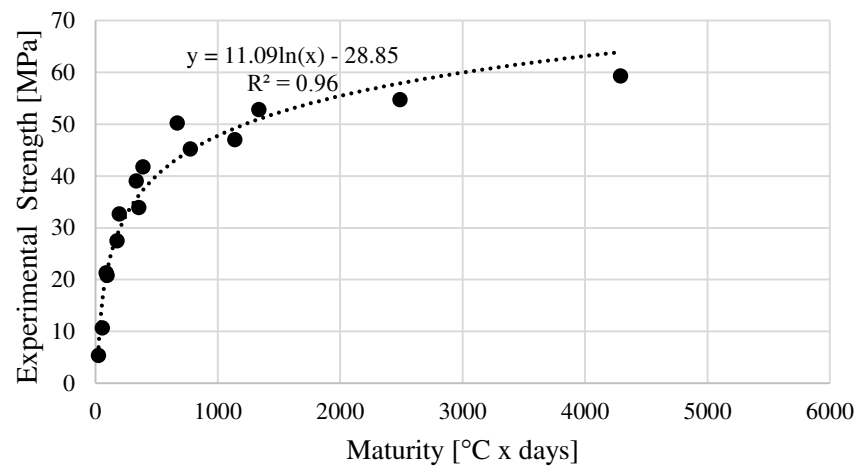


(b)

Figure 6.7 (a) Experimental strength-age (b) Experimental strength-maturity relationships for T-35 specimens

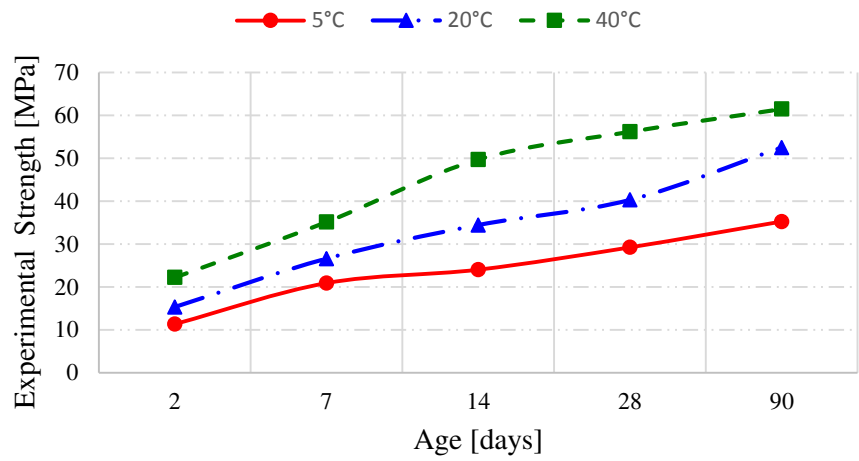


(a)

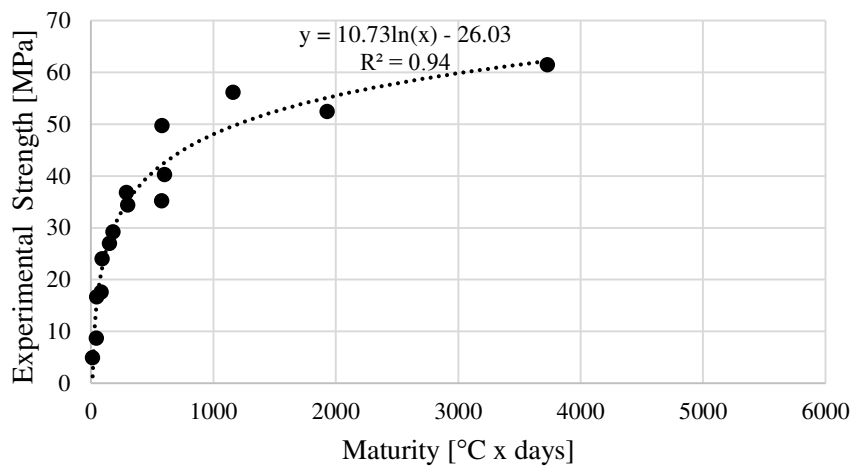


(b)

Figure 6.8 (a) Experimental strength-age (b) Experimental strength-maturity relationships for FA-6 specimens

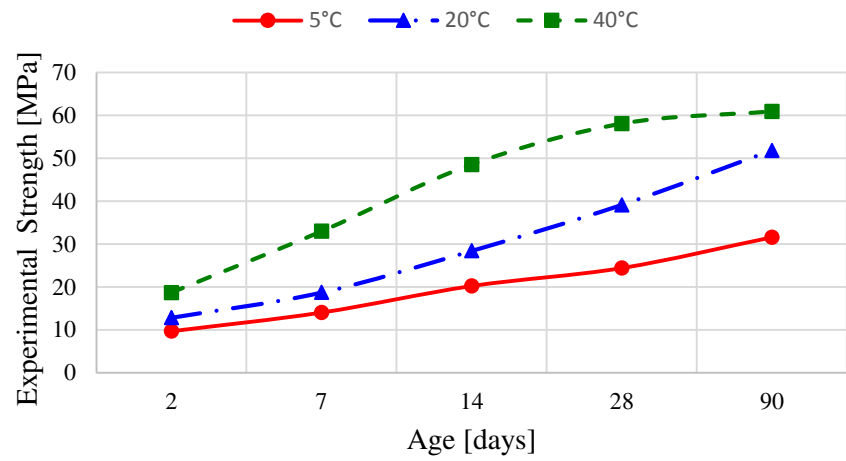


(a)

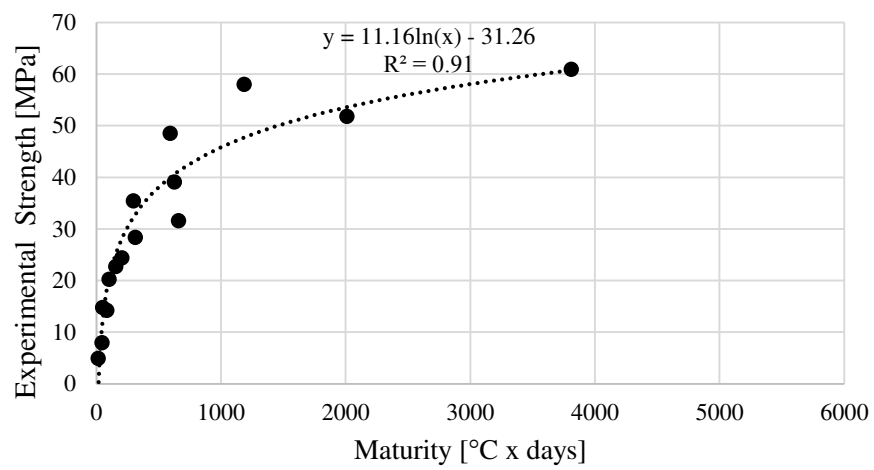


(b)

Figure 6.9 (a) Experimental strength-age (b) Experimental strength-maturity relationships for FA-20 specimens

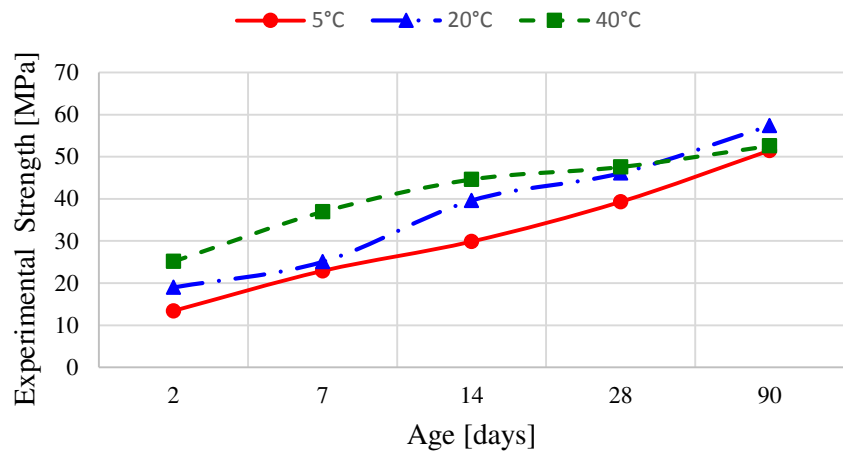


(a)

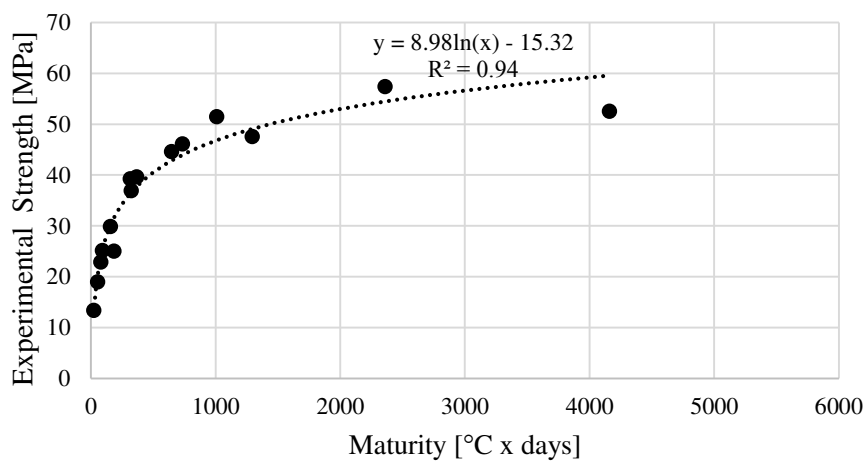


(b)

Figure 6.10 (a) Experimental strength-age (b) Experimental strength-maturity relationships for FA-35 specimens



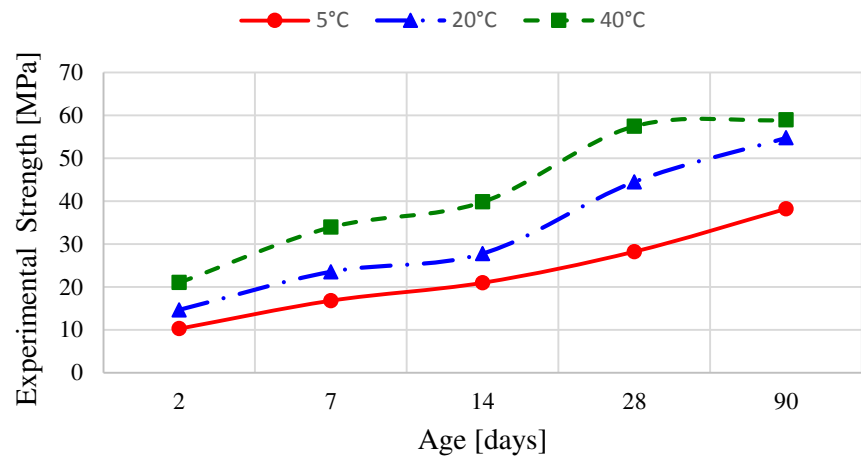
(a)



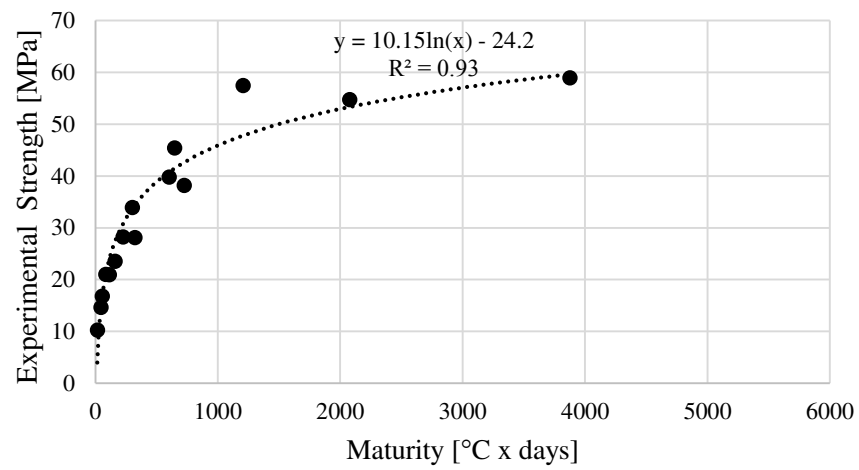
(b)

Figure 6.11 (a) Experimental strength-age (b) Experimental strength-maturity relationships for S-6 specimens



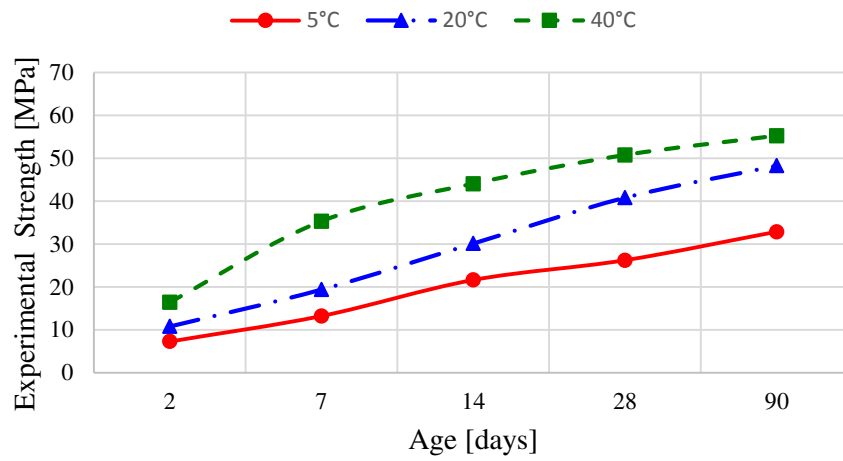


(a)

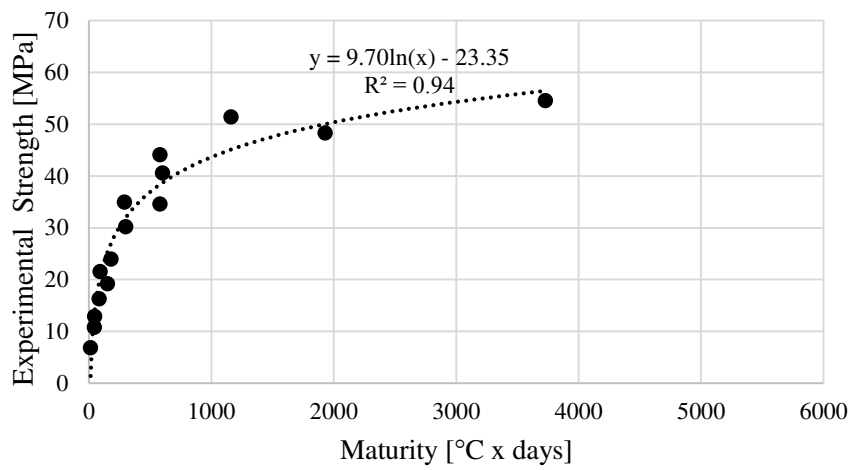


(b)

Figure 6.12 (a) Experimental strength-age (b) Experimental strength-maturity relationships for S-20 specimens



(a)



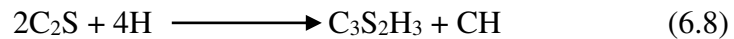
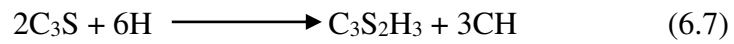
(b)

Figure 6.13 (a) Experimental strength-age (b) Experimental strength-maturity relationships for S-35 specimens

### 6.3. A New Approach for Examination of Datum Temperature and Apparent Activation Energy

The behavior of concretes at early and late ages may differ depending on the type and amount of mineral admixture incorporation. This is directly related with compounds of portland cement.

As Mehta and Monteiro (2006) explained in detail, as a result of hydration reactions of cement compounds, C-S-H and CH (notations that do not imply fixed chemical compositions) are obtained as shown below:



It can be inferred from stoichiometric calculations that  $C_3S$  produces 61 percent  $C_3S_2H_3$  and 39 percent CH, by mass while  $C_2S$  produces 82 percent  $C_3S_2H_3$  and 18 percent CH. Also, the irregularity of the arrangement of oxygen ions around calcium in Alite enables coordination of oxygen ions on one side of each calcium ions. This provides large structural holes which clarify its high lattice energy. On the other hand, interstitial holes in structure of belite are much smaller despite its irregular structure. This leads to less reactivity of belite. For these reasons, alite contributes to strength at early ages, whereas belite is mostly responsible for strength development at later ages (Mehta and Monteiro, 2006).

Increase in the strength development curve of the control portland cement specimens without any mineral admixtures gradually diminishes by time. This significantly increases the amount of energy to gain strength of mortars containing only portland cement at later ages.

Besides that, the effects of mineral admixtures on hydration were explained in detail in Chapter 3.2. Owing to these effects, especially pozzolanic reactions, an increase

in strength of mineral admixtures-incorporated mortars is generally expected in later ages by the consumption of portlandite obtained by hydration reactions. This is generally expected to reduce their  $E_a$  at later ages.

Due to the differences in the behavior of mortars with and without mineral admixtures at early and late ages,  $T_0$  and  $E_a$  values for each of mixtures were examined for early (2-7-14-day) and late ages (14-28-90-day) separately by considering A1.1.7 and A1.1.8.1 options stated in ASTM C 1074 and the results are shown in Table 6.6.

Table 6.6  $T_0$  and  $E_a$  values for each type of mixtures according to the new approach

Group	Option A1.1.7				Option A1.1.8.1			
	$T_0$ , °C (Early)	$E_a$ , J/mol (Early)	$T_0$ , °C (Later)	$E_a$ , J/mol (Later)	$T_0$ , °C (Early)	$E_a$ , J/mol (Early)	$T_0$ , °C (Later)	$E_a$ , J/mol (Later)
Control	-41.05	14727	2.34	38583	-10.91	22435	4.16	46332
LS-6	-70.34	10308	3.28	44965	-11.43	25648	3.28	38612
LS-20	-101.62	5422	-6.17	27631	-7.54	29181	-8.49	24246
LS-35	-16.97	19983	-8.72	23246	-6.92	30029	-4.81	25666
T-6	-76.76	6737	9.11	75028	-19.05	17977	9.06	55695
T-20	-47.66	10230	3.63	39782	-6.14	23981	4.26	40437
T-35	-695.00	1524	-4.56	25952	-5.38	25559	-1.62	28272
FA-6	5.05	52784	-5.64	30252	-8.68	24489	4.26	26411
FA-20	-1.08	32336	-28.13	13080	-0.97	28336	-12.44	17750
FA-35	-44.38	11096	-13.61	17149	-2.26	30905	-11.00	18506
S-6	-52.78	10604	-1.59	31944	-8.14	22755	-7.39	23576
S-20	-270.00	2553	-37.83	10394	-3.27	29351	-25.13	13853
S-35	-2299.00	245	-13.44	17996	-4.44	32845	-9.02	21237

Upon considering the results from Option A1.1.8.1, it may be said that when the  $E_a$  of mortars containing 6% mineral admixtures at early ages were compared with that of Control, only a small difference was found for LS-6 and T-6. It is thought that dilution effect is predominated in the 6% limestone incorporated mortar, while decrease in energy in 6% trass incorporated mortar is due to coarser trass particles. Due to less difference between the energies at early ages for the rest of all, incorporation of 6% mineral admixture into mortar is interpreted as having no major effect on the activation energies at early ages. At later ages, it can be noticeably seen that there occurred a considerable amount reduction in the activation energies for 6% replacement level of limestone, fly ash and GGBFS. For trass, its coarser particles prevents further pozzolanic reactions even if there may be sufficient amount of portlandite in the matrix. Thus, the minimum energy to gain strength in 6% trass added mortars is increased at later ages.

As the amount of mineral admixtures increases from 6% to 20-35%, an increase in activation energies of mortars containing mineral admixtures compared to that of the Control was observed at early ages except for trass incorporated mortars. The reason may be that mineral admixtures did not react with sufficient amount of portlandite in the matrix to form C-S-H gel at early ages since decrease in the amounts of alite and belite owing to the replacement of cement with mineral admixtures causes lesser amount of hydration products at early ages. On the other hand, there occurred a significant decrease in activation energies for 20% and 35% replacement level of mineral admixtures (other than trass) at later ages. The reason may be pozzolanic reactions.

#### **6.4. Development of A New Method for the Determination of Datum Temperature and Apparent Activation Energy**

Strength of the mortars without mineral admixtures asymptotically increases with time by approximating to the ultimate strength as shown Figure 6.14.

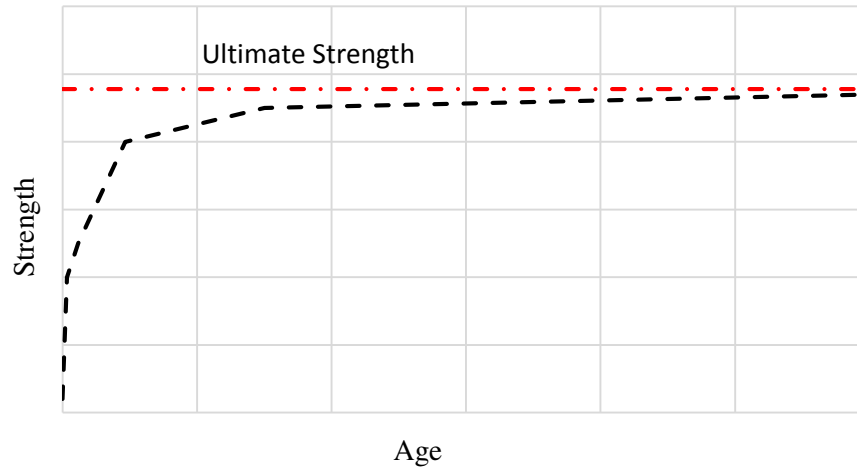


Figure 6.14 Strength development rate for mortars without mineral admixtures

As is seen from Figure 6.14, there is a logarithmic relationship between strength and age. Thus, the use of reciprocal of strength vs. reciprocal of natural logarithm of age beyond final setting times instead of reciprocal of age beyond final setting times in the Option A1.1.7 may better represent the behavior of the mortars. After plotting reciprocal of strength vs. reciprocal of natural logarithm of age beyond final setting time, coefficients of the natural logarithm gives “T-values”. The steps followed for determination of  $T_0$  and  $E_a$  are completely same as those in Option A1.1.7.  $T_0$  and  $E_a$  values obtained by using new method for each type of mixture are shown in Table 6.7.

Table 6.7  $T_0$  and  $E_a$  values for each type of mixtures according to  
proposed method

Group	$T_0$ , °C	$E_a$ , J/mol
Control	-9.94	23621
LS-6	-19.30	20282
LS-20	-28.35	14476
LS-35	-15.14	21637
T-6	-13.66	20319
T-20	-11.88	21801
T-35	-17.20	19658
FA-6	-1.12	34301
FA-20	-3.35	29952
FA-35	-9.56	23517
S-6	-15.33	19835
S-20	-21.91	16591
S-35	-15.30	20021

The procedures and the calculations of  $T_0$  and  $E_a$  for the proposed method are explained by an example in Appendix C.

## 6.5. Equivalent Age Functions

In this chapter, equivalent age-strength rate relationship for each type of mixture is shown in Figure 6.15 to Figure 6.27. As equivalent age function, Equation (2.6) is used throughout the calculations. Besides, 20°C is accepted as reference for equivalent age functions and relative strength calculations (say strength at 5°C divided by strength at 20°C for and strength at 40°C divided by strength at 20°C) for each test age (2, 7, 14, 28 and 90-day)



It is assumed that the strength converges to limiting strength as time passes whatever curing temperature (5°C, 20°C or 40°C) is used. The assumption can be easily seen from Figure 6.15,

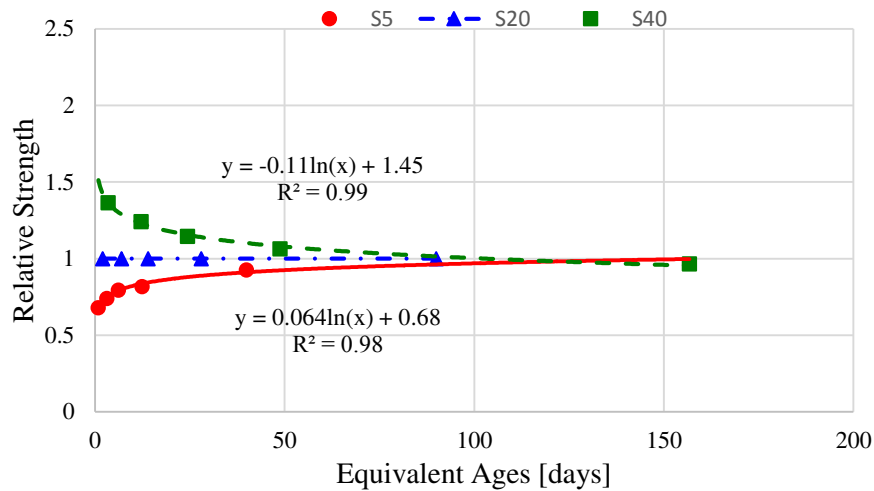


Figure 6.15 Strength rate-equivalent age for Control specimens

It is also inferred from the Figure 6.15 that the curve for the mortars without additives cured at 40°C has higher degree of divergence than those cured at 5°C especially at early ages. The reason may be acceleration effect of 40°C on hydration reactions.

On the other hand, mineral admixture-incorporated mortars behave differently from mortars without any additives. As the amount of mineral admixtures increases, a straight line having a slope approaching zero is obtained especially at 5°C. However, regardless of increase in the amount of mineral admixtures, mortars cured at 40°C display approximately similar behavior with mortars without additives cured at 40°C.

It can be inferred from strength development rate-equivalent age curves that limiting strength for mixtures with merely portland cement may be independent of selected curing temperatures whereas it can be recommended from results of mixes with additives that the use of limiting strength at low curing temperature (5°C) is not suitable for other curing temperatures (20°C and 40°C).

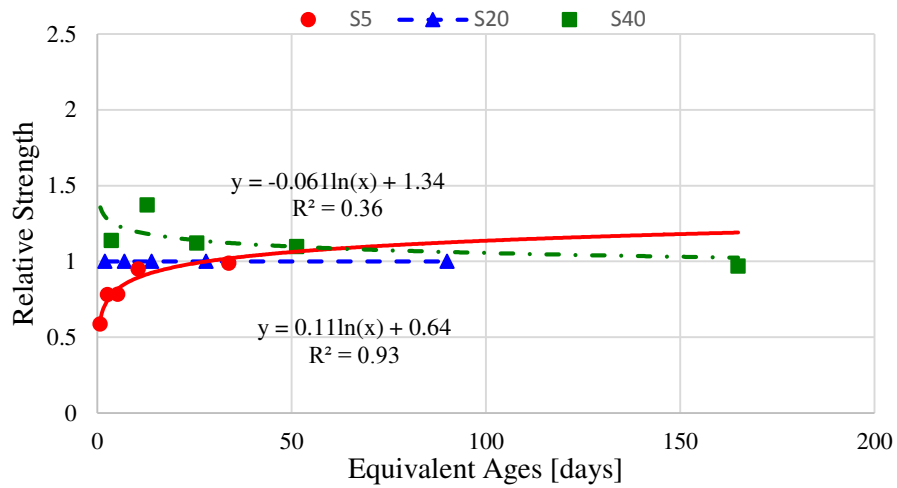


Figure 6.16 Relative strength-equivalent age for LS-6 specimens

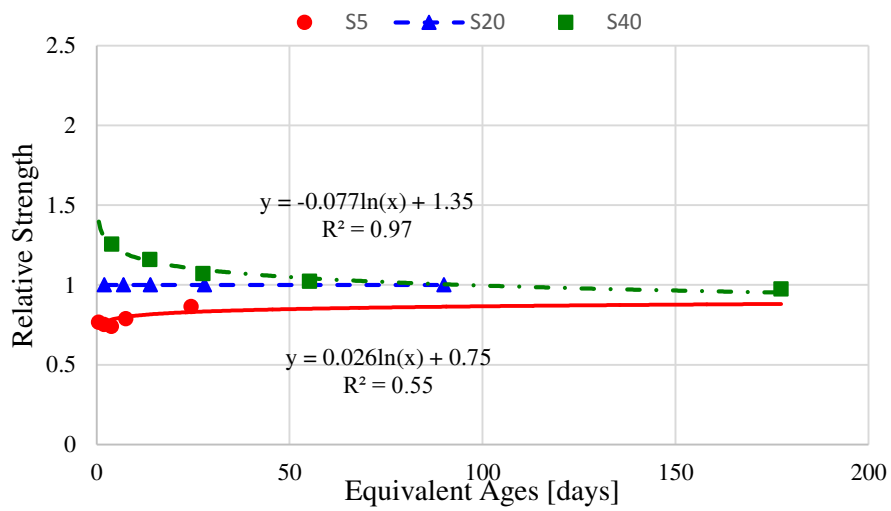


Figure 6.17 Relative strength-equivalent age for LS-20 specimens

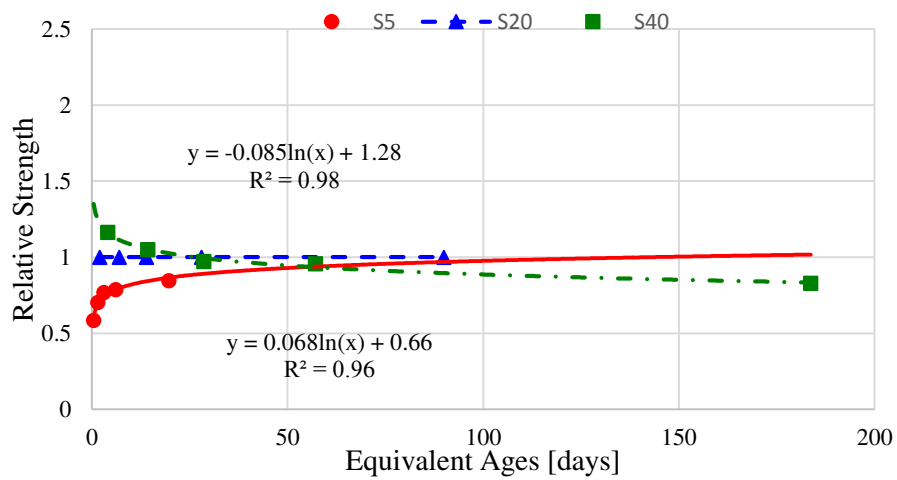


Figure 6.18 Relative strength-equivalent age for LS-35 specimens

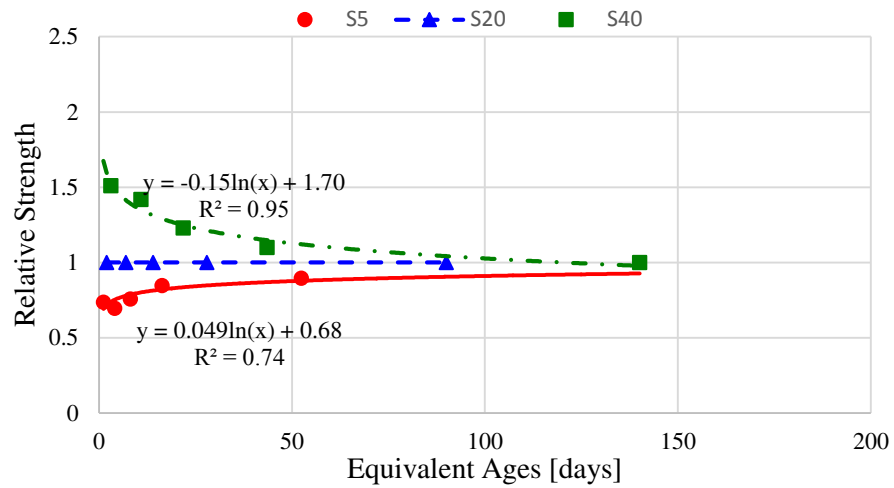


Figure 6.19 Relative strength-equivalent age for T-6 specimens

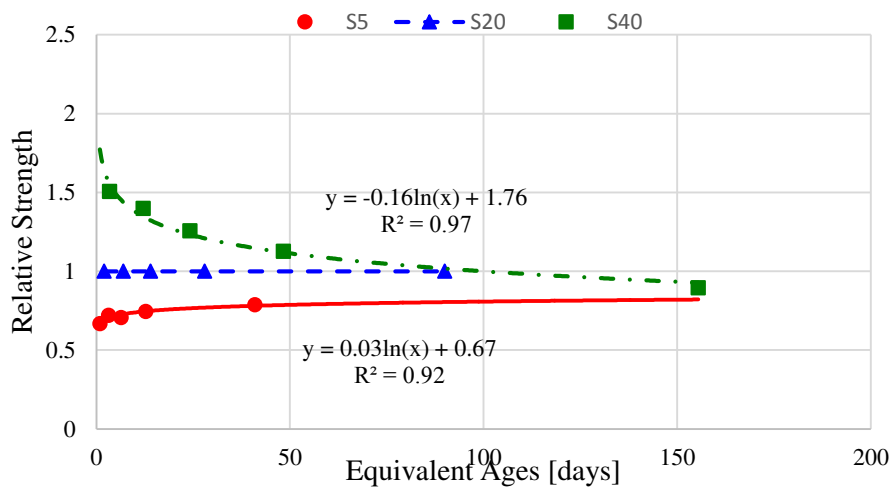


Figure 6.20 Relative strength-equivalent age for T-20 specimens

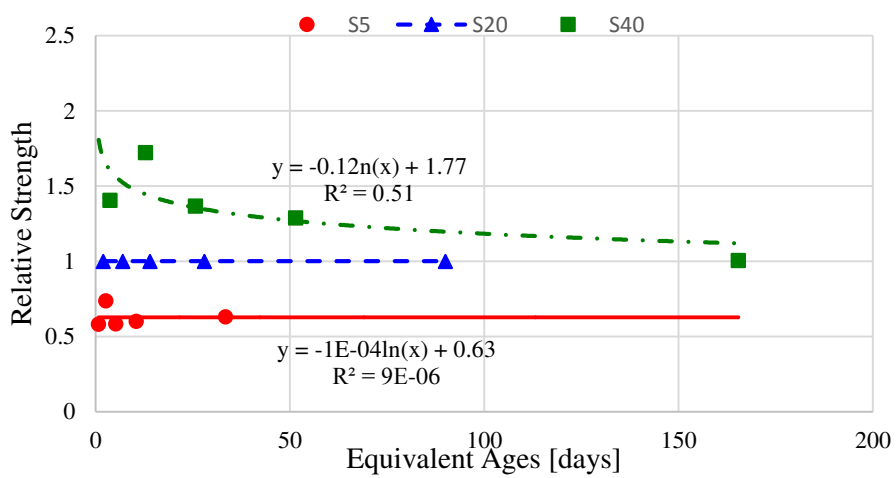


Figure 6.21 Relative strength-equivalent age for T-35 specimens

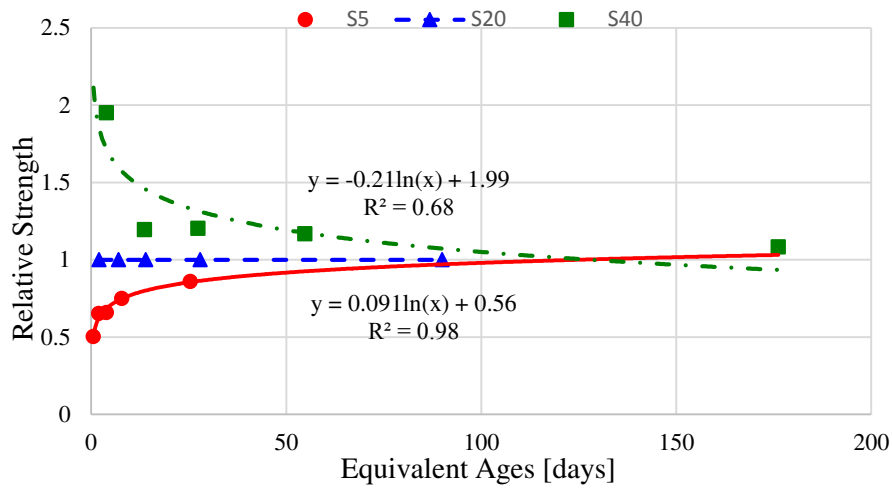


Figure 6.22 Relative strength-equivalent age for FA-6 specimens

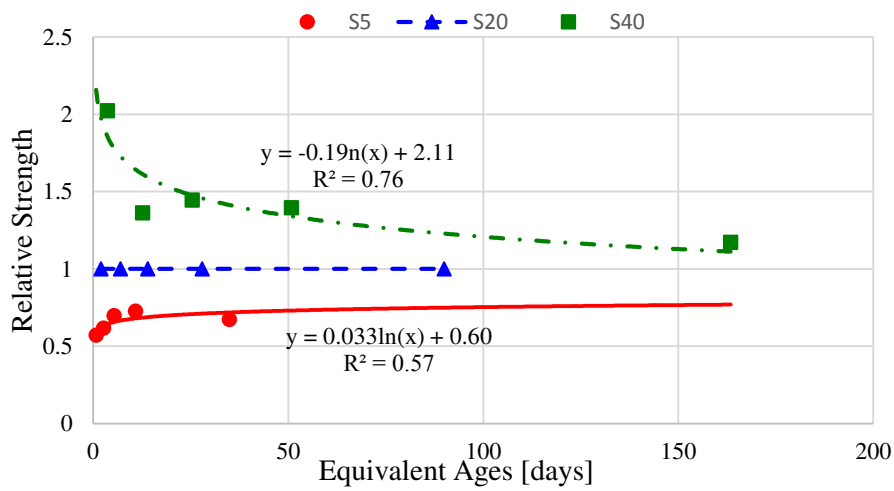


Figure 6.23 Relative strength-equivalent age for FA-20 specimens

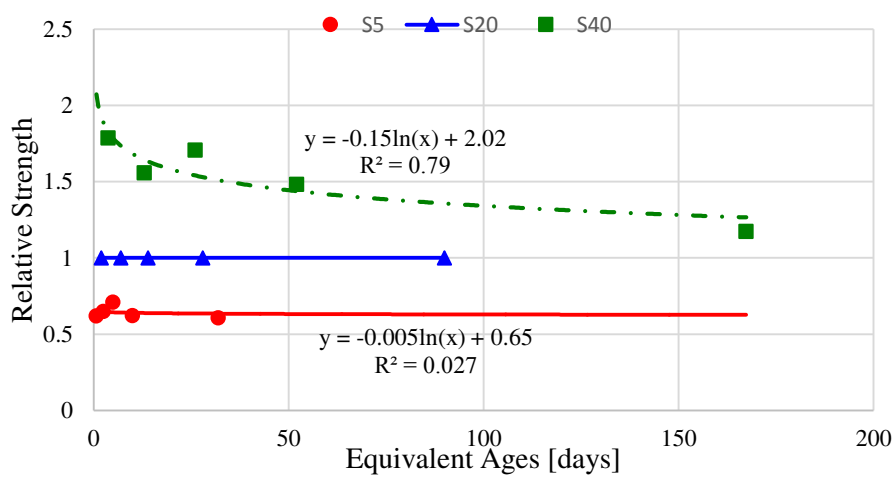


Figure 6.24 Relative strength-equivalent age for FA-35 specimens

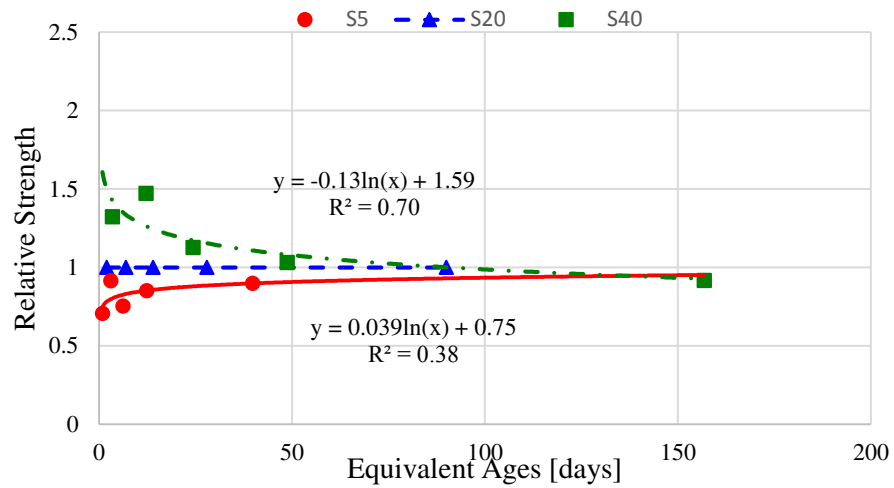


Figure 6.25 Relative strength-equivalent age for S-6 specimens

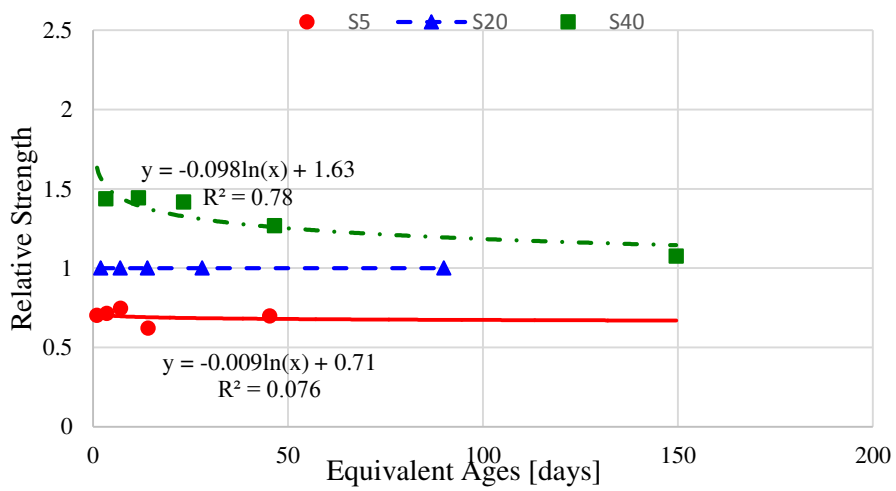


Figure 6.26 Relative strength-equivalent age for S-20 specimens

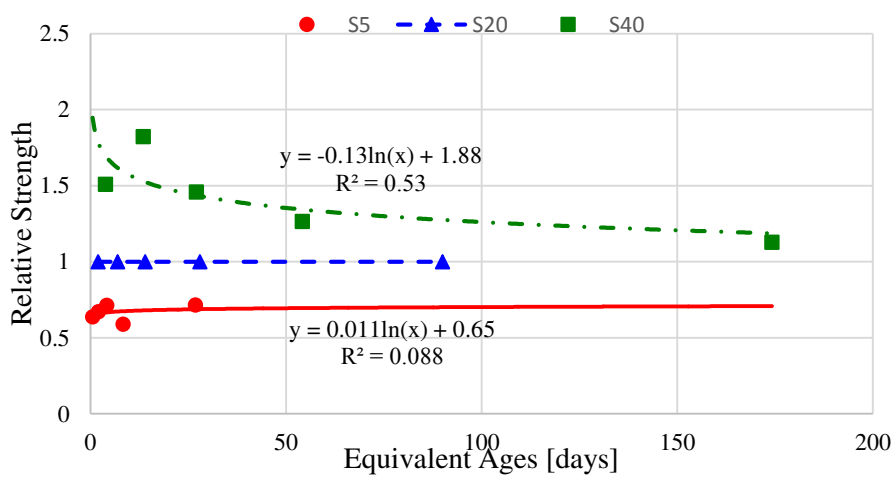


Figure 6.27 Relative strength-equivalent age for S-35 specimens



## CHAPTER 7

### CONCLUSIONS

This study has been conducted to investigate the effect of mineral admixture-incorporated mortars on the maturity and equivalent age functions. For this purpose, mortars were prepared by using four different mineral admixtures (limestone, trass, fly ash and GGBFS) at different percentages (6, 20 and 35% by weight). Also, control mortars without mineral admixture were prepared to follow the effect of mineral admixtures. All mortars were cured at three different temperatures (5°C, 20°C and 40°C). Then, compressive strength of the mortars was tested at 2, 7, 14, 28 and 90-day.

From the discussion and test results in this study, the following conclusions are drawn:

- Option A1.1.8.1 among methods in ASTM C1074 may best define behavior of mineral admixture-incorporated mortars to calculate  $T_0$  and  $E_a$ . However, especially at later ages, the determination of  $T_0$  and  $E_a$  for these mortars may not give correct results due to pozzolanic reactions.
- Experimental strength—maturity and experimental strength—predicted strength relationships for each type of mixture can be fairly established.
- Evaluation of  $T_0$  and  $E_a$  values at early and later ages separately by using the proposed approach obtained by utilizing Option A1.1.8.1 may be more appropriate.

- Proposed method adapted from Option A1.1.7. comprises behavior of mortars with mineral admixtures at early and later ages. Thus, it may be used as an alternative as well as methods in ASTM C1074 to determine  $T_0$  and  $E_a$ .
- From equivalent age-strength rate development relationships for all mortars with mineral admixtures, limiting strength is not independent of curing temperatures. Calculation of a separate limiting strength at 5°C, which differs from that of 20°C and 40°C, is necessary. However, there is no significant difference between that of 20°C and 40°C.



## REFERENCES

- Abdel-Jawad, Y.A. (2006). The maturity method: modifications to improve estimation of concrete strength at later ages. *Construction and Building Materials*, 20 (10): 893–900.
- ACI 308. (2001). "Guide to Curing Concrete". ACI Committee 308 Report, ACI 308R-01, American Concrete Institute, Farmington Hills, MI.
- Alonso, J.L. And Wesche, K. (1991). Characterization of fly ash. In "Fly Ash in Concrete Properties and Performance". K. Wesche (Ed), E&FN Spon, London.
- ASTM C125. (2003). "Standard Terminology Relating to Concrete and Concrete Aggregates." ASTM, 100 Barr Harbor Drive, West Conshohocken, PA.
- ASTM C618. (2012). "Standard Specification for Coal Fly Ash and Raw or Calcined Natural Pozzolan for Use." ASTM, 100 Barr Harbor Drive, West Conshohocken, PA.
- ASTM C1074. (2011). "Standard Practice Estimating Concrete Strength by the Maturity Method." ASTM, 100 Barr Harbor Drive, West Conshohocken, PA.
- Barnett, S. J., Soutsos, M. N., Millard, S. G., and Bungey, J. H. (2006). Strength development of mortars containing ground granulated blast-furnace slag: Effect of curing temperature and determination of apparent activation energies. *Cement and Concrete Research*, 36(3): 434–40.
- Bergstrom, S. G. (1953). Curing temperature, age and strength of concrete. *Magazine of Concrete Research*, 5(14): 61–66.
- Bernhardt, C. J. (1956). Hardening of concrete at different temperatures. In "Proceedings of the RILEM Symposium on Winter Concreting", Copenhagen.
- Boubekeur, T., Ezziane, K., and El Hadj K. (2014). Estimation of mortars compressive strength at different curing temperature by the maturity method. *Computers and Chemical Engineering*, 71: 299–307.

- Carino, N. J. (1984). The maturity method: theory and application. *Cement, Concrete and Aggregate*, 6(2): 61–73.
- Carino, N. J., and Lew, H. S. (2001). “The Maturity Method: From Theory to Application.” Structures 2001 Structural Engineering Odyssey, 1–19.
- Carino, N. J. (1997). Nondestructive test methods. In "Concrete Construction Engineering Handbook". E. G. Nawy (Ed), CRC Press, New York.
- CSI (2005). "Guidelines for the Selection and Use of Fuels and Raw Materials in the Cement Manufacturing Process". World Business Council for Sustainable Development, Geneva.
- Damtoft, J. S., Herfort, D. S., and Gartner, E. M. (2008). Sustainable development and climate change initiatives. *Cement and Concrete Research*, 38: 115–27.
- Dhir, R. K. (1986). Pulverized-fuel ash. In "Cement Replacement Materials" R.N.Swamy, (Ed). Surrey University Press, Guildford, Surrey, UK.
- EN 197-1. (2012). “Cement Part 1: Composition, Specifications and Conformity Criteria for Common Cements.” CEN, Brussels.
- Erdoğan, K. (2002). “Hydration Properties of Limestone Incorporated Cementitious Systems.” Middle East Technical University, PhD Thesis, Ankara, 115pp.
- Eren, Ö. (2002). Strength development of concretes with ordinary portland cement, slag or fly ash cured at different temperatures. *Materials and Structures*, 35: 536–40.
- Ferreira, L., Branco, F., Costa, H., Julio, E., Maranha, P. (2015). Characterization of alkali-activated binders using the maturity method. *Construction and Building Materials*, 95: 337–44.
- Gartner, E. (2004). Industrially interesting approaches to ‘Low-CO<sub>2</sub>’ cements. *Cement and Concrete Research*, 34: 1489–98.
- Halse, Y., Pratt, P.L., Dalziel, J.A. and Gutteridge, W.A. (1984). Development of microstructure and other properties in fly ash OPC systems. *Cement and Concrete Research*, 491–98.

- Hansen, F. and Pedersen, E.J. (1977). Maturity Computer for Controlled Curing and Hardening of Concrete. *Nordisk Betong*, V.1: 19–34.
- Kasap, O. (2002). "Effects of Cement Type on Concrete Maturity". Middle East Technical University, M.S. Thesis, Ankara. 98pp.
- Knudsen, T. (1980). On particle size distribution in cement hydration. *proc. 7th Int. Congr. Chem. Cement*, II,I: 170–75.
- Lawrence, P., Martin, C., and Ringot, E. (2003). Mineral admixtures in mortars. *Cement and Concrete Research* ,33: 1939–47.
- Lee, C. H., and Hover, K.C. (2015). Influence of datum temperature and activation energy on maturity strength predictions. *ACI Materials Journal*, 112(M74): 781–90.
- Lothenbach, B., Scrivener, K., and Hooton. R.D. (2011). Supplementary cementitious materials.” *Cement and Concrete Research* 41: 1244–56.
- Malhotra, V. M., Carino, N. J. (2004). “Handbook on Nondestructive Testing of Concrete.” CRC Press: Boca Raton, Florida.
- Massazza, F. (1988). Pozzolona and pozzolanic cements. In "Lea's Chemistry of Cement and Concrete" P.C. Hewlett (Ed), Elsevier, Oxford.
- McIntosh, J. (1949). Electrical curing of concrete. *Magazine of Concrete Research*, 1: 21–28.
- Mehta, P. K., Monteiro, P.J.M. (2006). "Concrete Microstructure, Properties and Materials". 3rd Ed., McGraw-Hill, New York.
- Moranville-Regourd, M. (2006). Cements made from Blastfurnace Slag. In "Lea's Chemistry of Cement and Concrete". 4th ed., Hewlett, P. C. (Ed), Butterworth-Heinemann, Elsevier, Oxford.
- Nixon, J. M., Anton K. Schindler, A. K., Robert W. B., and Wade, S. A. 2008. Evaluation of the maturity method to estimate concrete strength in field applications.” Alabama Department of Transportation, ALDOT Project 930-590, p. 309.

- Nurse, R.W. (1949). Steam curing of concrete. *Magazine of Concrete Research*, 1(2): 79–88.
- Odler, I. (2000). Cements containing ground granulated blast furnace slag. In "Special Inorganic Cements". Spon, E.&F.N., London.
- Özdemir, O. (2001). "Characterization and Recovery of Tunçbilek Power Station Fly Ash by-Products". Istanbul Technical University, M.S. Thesis, Istanbul, 96pp.
- Plowman, J. M. (1956). Maturity and the strength of concrete. *Magazine of Concrete Research*, (22): 13–22.
- Ramachandran, V. S. (1995). "Concrete Admixtures Handbook." Noyes Publications, New Jersey.
- Rastrup, E. (1954). Heat of hydration in concrete. *Magazine of Concrete Research*, 79–92.
- Regourd, M., Thomassin, J.H., Baillif, P. and Touray, J.C. (1983). Blast furnace slag hydration. *Cement and Concrete Research*, 13(4): 549–56.
- Saul, A.G.A. (1951). Principles underlying the steam curing of concrete at atmospheric pressure. *Magazine of Concrete Research*, 2(6): 127–40.
- Shukla, M. K., Mishra, S.P. (2015). In place strength of cement mortar/concrete using maturity and activation energy. *International Journal of Advanced Engineering Research and Studies*, IV/II: 79–82.
- Tokyay, M., Erdoğan, K. (1998). "Characterization of Turkish Fly Ashes." TÇMB/AR-GE/Y 98.3, Turkish Cement Manufacturers' Association, 70.
- Tokyay, M. (2016). "Cement and Concrete Mineral Admixtures." CRC Press, Taylor & Francis Group, London.
- Vázquez-Herrero, C., Martínez-Lage, I., and Sánchez-Tembleque, F. (2012). A new procedure to ensure structural safety based on the maturity method and limit state theory. *Construction and Building Materials*, 35: 393–98.

- Voigt, T., Sun, Z. and Shah, S. P. (2006). Comparison of ultrasonic wave reflection method and maturity method in evaluating early-age compressive strength of mortar. *Cement and Concrete Composites*, 28(4): 307–16.
- Yikici, T. A., Chen, H. (2015). Use of maturity method to estimate compressive strength of mass concrete. *Construction and Building Materials*, 95: 802–12.
- Zhang, J., Cusson, D., Monteiro, P., Harvey, J. (2008). New perspectives on maturity method and approach for high performance concrete applications. *Cement and Concrete Research*, 38(12): 1438–46.



## APPENDICES

### APPENDIX A

#### DETERMINATION OF DATUM TEMPERATURE AND APPARENT ACTIVATION ENERGY ACCORDING TO OPTIONS A1.1.7, A1.1.8.1, AND A1.1.8.2

All data used through the calculations was obtained from the Control mixtures.

##### A1. Determination of Datum Temperature and Apparent Activation Energy According to Option A1.1.7

Table A.1 Experimental compressive strength test results and age beyond final  
setting time for Control specimens

Age [days]	Compressive Strength [MPa]			Age Beyond Final Setting Time [days]
	5°C	20°C	40°C	20°C
2	14.13	20.82	28.42	1.79
7	24.47	33.02	41.02	6.79
14	32.53	40.90	46.87	13.79
28	38.35	46.95	49.93	27.79
90	48.27	52.15	50.42	89.79

Table A.2 Reciprocal age beyond final setting time and reciprocal experimental compressive strength results for Control specimens

Reciprocal Age Beyond Final Setting Time [1/days]	Reciprocal Compressive Strengths [1/MPa]		
	5°C	20°C	40°C
20°C	5°C	20°C	40°C
0.560	0.071	0.048	0.035
0.150	0.041	0.030	0.024
0.073	0.031	0.025	0.021
0.036	0.026	0.021	0.020
0.011	0.021	0.019	0.019

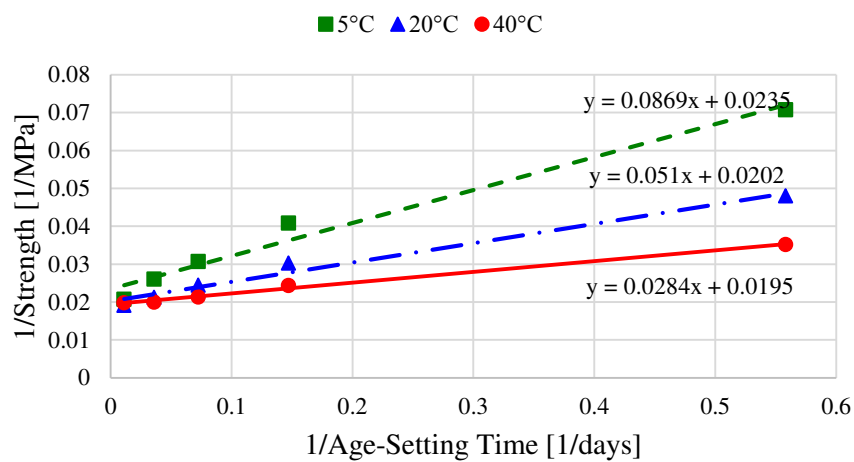


Figure A.1 Reciprocal of experimental strength vs. reciprocal of age beyond time of final setting for Control specimens in Option A1.1.7

k-values at the three temperatures for Option A1.1.7 were determined by dividing the value of the intercept by the value of slope for each straight-line in Figure A.1, and the results are summarized in Table A.3.



Table A.3 k-values at each temperature in Option A1.1.7 for Control specimens

Curing Temperature [°C]	k [-]
5	0.27
20	0.40
40	0.69

To determine  $T_0$ , k-values vs. temperature are plotted as Figure A.2.

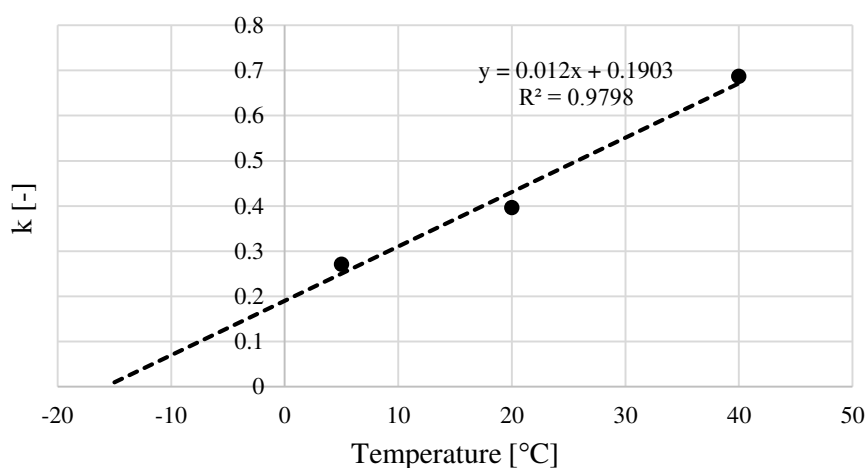


Figure A.2 k-values vs. curing temperature for Control specimens in Option A1.1.7

$T_0$  is the point where the straight line cuts the x-axis. Thus,  $T_0$  for Control in Option A1.1.7 is  $-15.86^{\circ}\text{C}$ .

Table A.4 Reciprocal curing temperature and natural logarithm of k-values for Control specimens

1/Curing Temperatures [1/°K]	ln(k) [-]
0.0036	-1.31
0.0034	-0.93
0.0032	-0.38

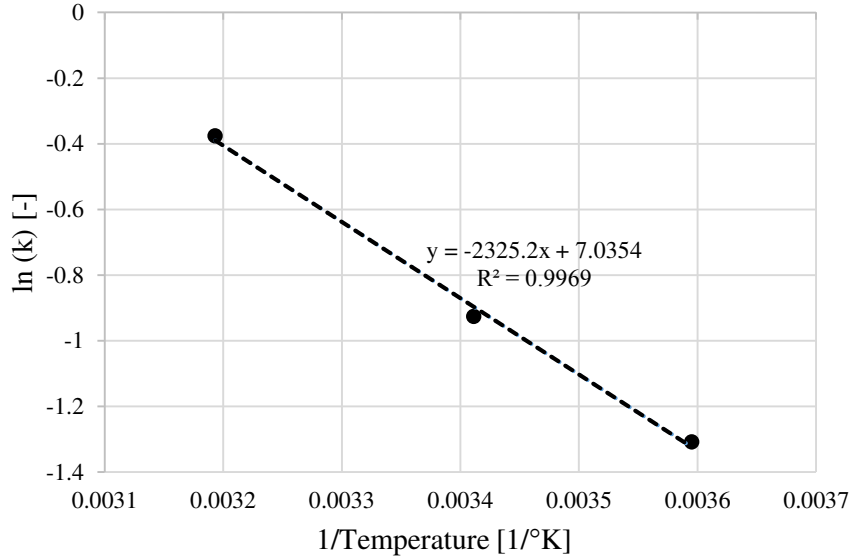


Figure A.3 Natural logarithm of k-values vs. inverse absolute temperature for Control specimens in Option A1.1.7

Slope of the straight line is equal to  $-E_a/R$ , where R is gas constant.  $E_a$  for Control in Option A1.1.7 is 19283 J/mol.

## A2. Determination of Datum Temperature and Apparent Activation Energy According to Option A1.1.8.1

$S_u$ ,  $k_T$ , and  $t_0$  values at each temperature for Control were calculated using Equation (2.9). The equation is written separately for each age. A system of five equations with three unknowns is obtained. An easy way for solving the system is to use a tool such as Excel Solver. The system is solved via Excel Solver and the results are as in Table A.5.

Table A.5  $S_u$ ,  $k_T$ , and  $t_0$  values at each temperatures for Control specimens

Age [days]	Compressive Strength [MPa]		
	5°C	20°C	40°C
$S_u$	52.62	55.44	54.29
$k_T$	0.122	0.174	0.398
$t_0$	0.715	0.354	0.178

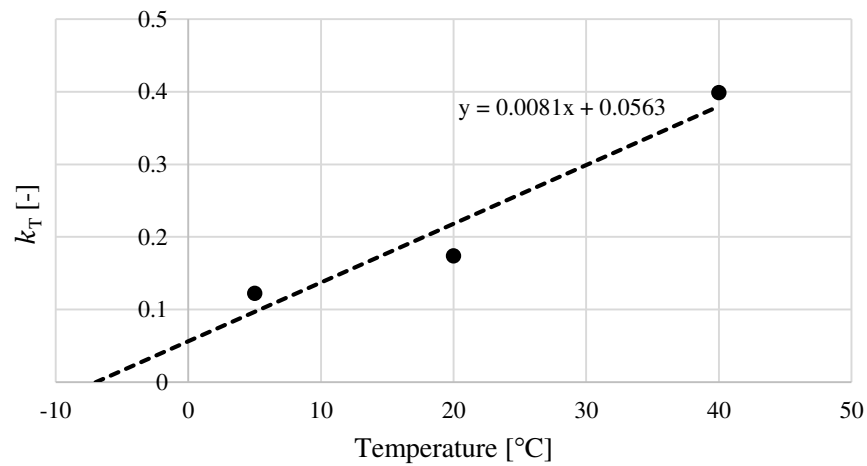


Figure A.4  $k_T$ -values vs. curing temperature for Control specimens in Option A1.1.8.1

$T_0$  is the point where the straight line cuts the x-axis. Thus,  $T_0$  for Control in Option A1.1.8.1 is -6.95°C.

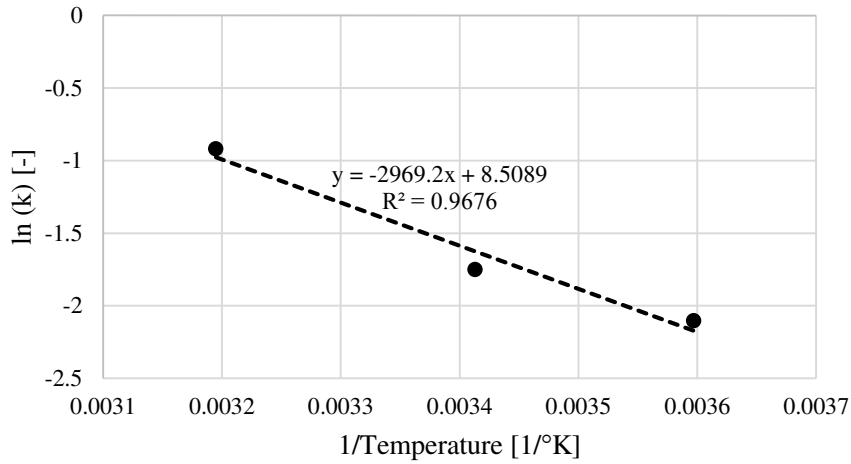


Figure A.5 Natural logarithm of k-values vs. inverse absolute temperature for  
Control specimens in Option A1.1.8.1

Slope of the straight line is equal to  $-E_a/R$ , where R is gas constant.  $E_a$  for Control in Option A1.1.8.1 is 24686 J/mol.

### A3. Determination of Datum Temperature and Apparent Activation Energy According to Option A1.1.8.2

Reciprocal of strength vs. reciprocal of age for Control was plotted by using data from last four test ages as Figure A.6.

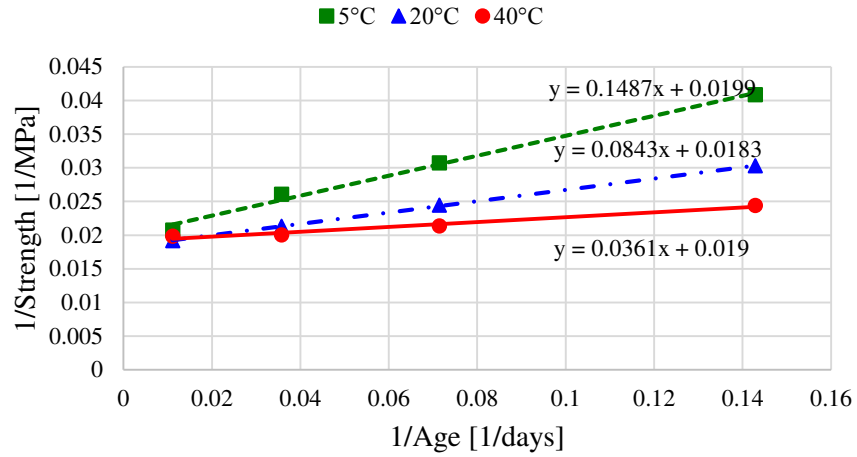


Figure A.6 Reciprocal of strength vs. reciprocal of age for Control specimens in Option A1.1.8.2

y-axis intercepts were determined for each temperature. The inverses of the intercepts were the limiting strengths,  $S_u$  for each temperature. The intercepts and the limiting strengths were shown in Table A.6.

Table A.6  $S_u$  values at each temperatures for Control specimens

Curing Temperatures [°C]	y-axis intercepts	Limiting Strength, $S_u$ [MPa]
5	0.0199	50.25
20	0.0183	54.64
40	0.0190	52.63

After determining limiting strength,  $S_u$ , A-values for first four test ages at three different temperatures were calculated by using Equation (2.20), and the results are shown in Table A.7.

Table A.7 A-values for first four test ages at three different temperatures for Control specimens

Age [days]	A-values [-]		
	5°C	20°C	40°C
2	0.39	0.62	1.17
7	0.95	1.53	3.53
14	1.84	2.98	8.14
28	3.22	6.10	18.48

As mentioned in Chapter 2.3., k-values at each curing temperature in the Option A1.1.8.2 can be determined by using A vs. Age plot. The slope of best-fit straight lines at each curing temperatures gives k-value. Therefore, A-values vs. Age were plotted in Figure A.7, and the results were shown in Table A.8.

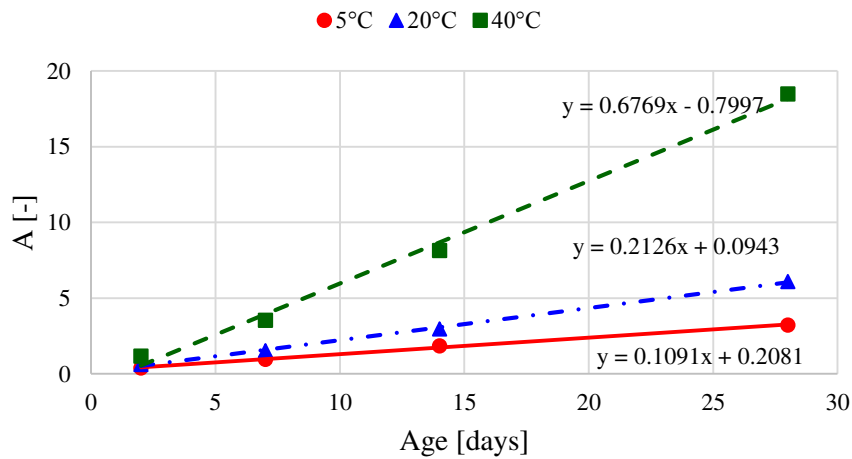


Figure A.7 Reciprocal of strength vs. reciprocal of age for Control specimens in Option A1.1.8.2

Table A.8 k-values at each curing temperatures in Option A1.1.8.2 for Control specimens

Curing Temperature [°C]	k [-]
5	0.1091
20	0.2126
40	0.6769

To figure out  $T_0$ , k-values vs. curing temperatures was plotted as Figure A.8.

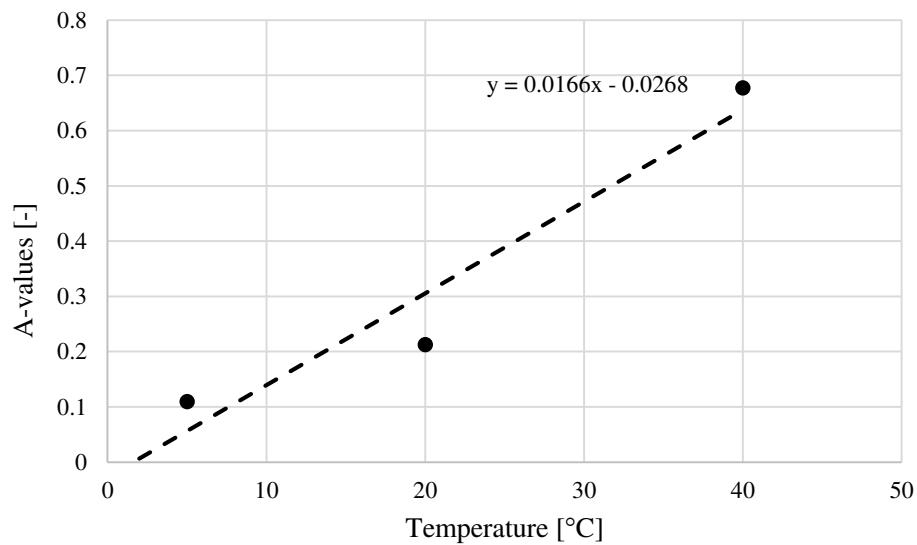


Figure A.8 Reciprocal of strength vs. reciprocal of age for Control specimens in Option A1.1.8.2

$T_0$  is the point where the straight line cuts the x-axis. Thus,  $T_0$  for Control in Option A1.1.8.2 is 1.61°C.

Table A.9 Reciprocal curing temperature and natural logarithm of k-values for  
Control specimens

1/Curing Temperatures [1/°K]	ln(k) [-]
0.003595	-2.22
0.003411	-1.55
0.003193	-0.39

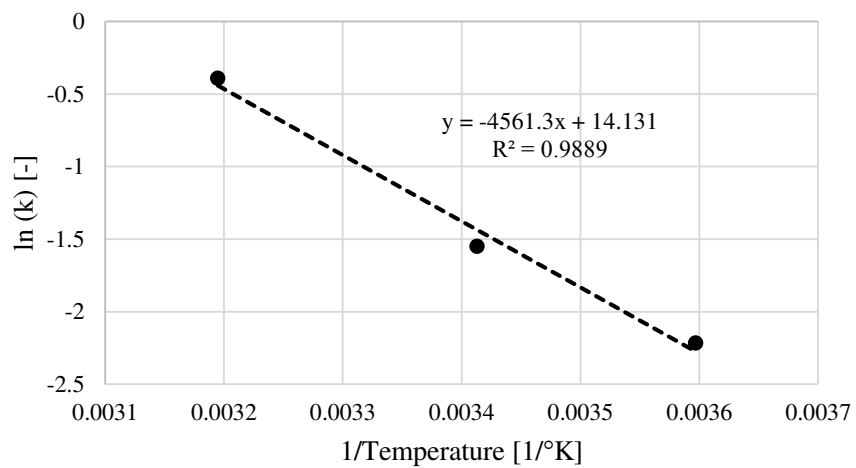


Figure A.9 Natural logarithm of k-values vs. inverse absolute temperature for  
Control specimens in Option A1.1.8.2

Slope of the straight line is equal to  $-E_a/R$ , where R is gas constant.  $E_a$  for Control in Option A1.1.8.2 is 37923 J/mol.



## APPENDIX B

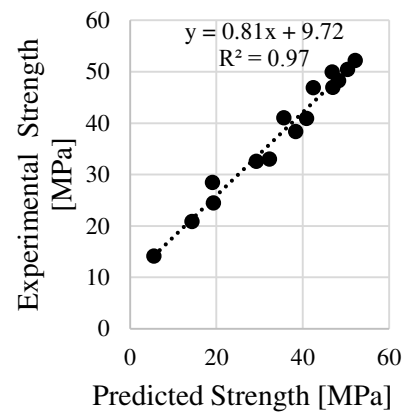
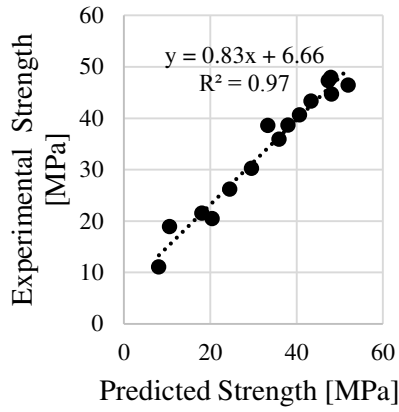
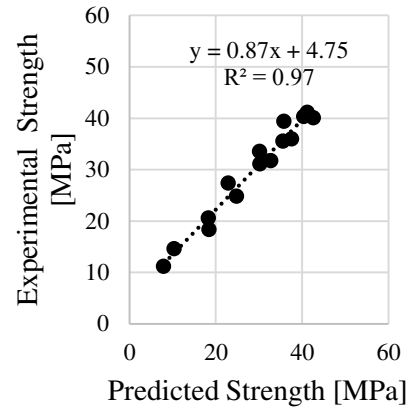


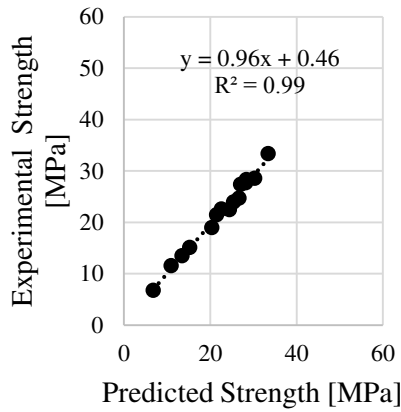
Figure B.1 Experimental strength vs. predicted strength for Control specimens



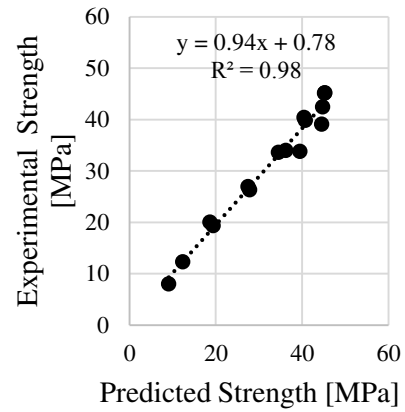
(a)



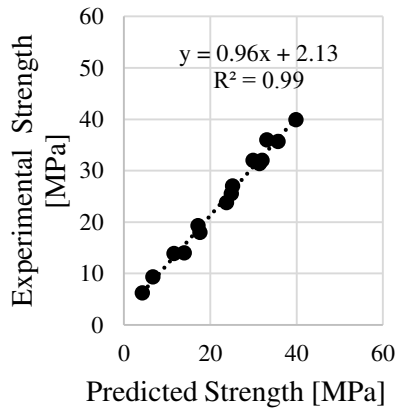
(b)



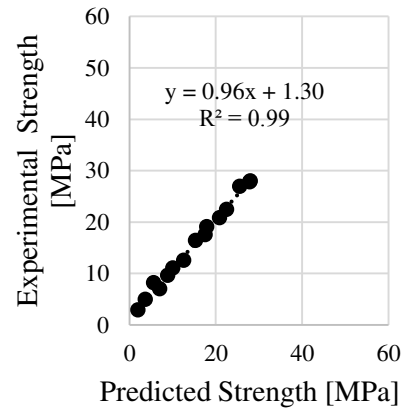
(c)



(d)

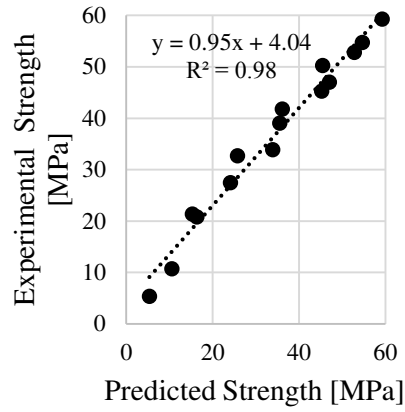


(e)

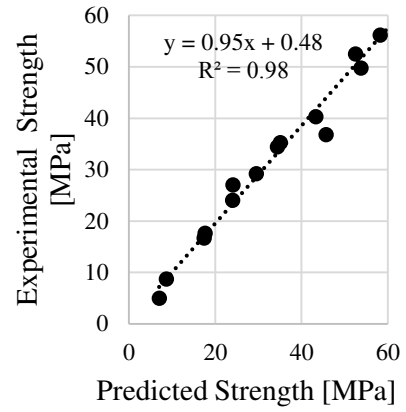


(f)

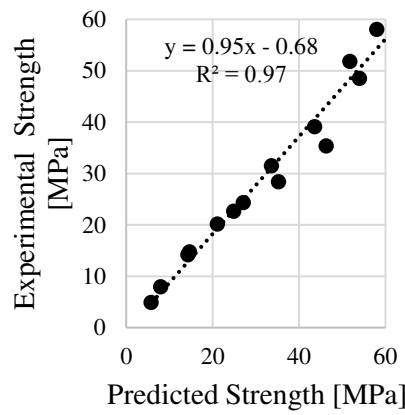
Figure B.2 Experimental strength vs. predicted strength for (a) LS-6, (b) LS-20, (c) LS-35, (d) T-6, (e) T-20, (f) T-35 specimens



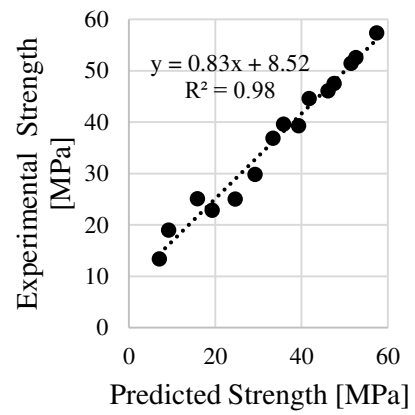
(a)



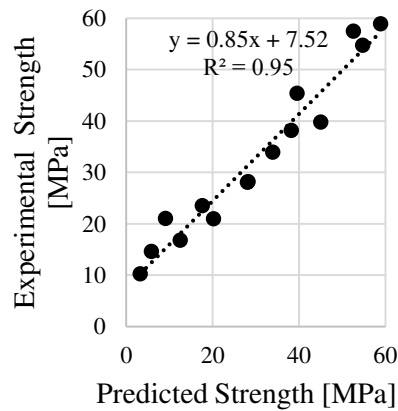
(b)



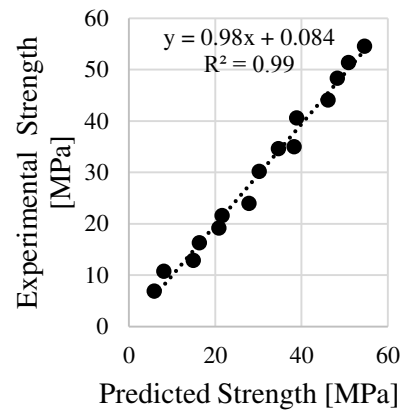
(c)



(d)



(e)



(f)

Figure B.3 Experimental strength vs. predicted strength for (a) FA-6, (b) FA-20, (c) FA-35, (d) S-6, (e) S-20, (f) S-35 specimens

## APPENDIX C

Table C.1 Compressive strength test results and reciprocal natural logarithm of age beyond final setting time at 20°C for Control specimens

Age [days)	Compressive Strength [MPa]			Natural Logarithm of Age Beyond Final Setting Time at 20°C [days]
	5°C	20°C	40°C	
2	14.13	20.82	28.42	0.58
7	24.47	33.02	41.02	1.92
14	32.53	40.9	46.87	2.62
28	38.35	46.95	49.93	3.33
90	48.27	52.15	50.42	4.50

Table C.2 Reciprocal natural logarithm of age beyond final setting time at 20°C and reciprocal experimental compressive strength results for Control specimens

Reciprocal Natural Logarithm of Age Beyond Final Setting Time at 20°C [1/days]	Reciprocal Compressive Strengths [1/MPa]		
	5°C	20°C	40°C
1.72	0.071	0.048	0.035
0.52	0.041	0.030	0.024
0.38	0.031	0.025	0.021
0.30	0.026	0.022	0.020
0.22	0.021	0.019	0.020

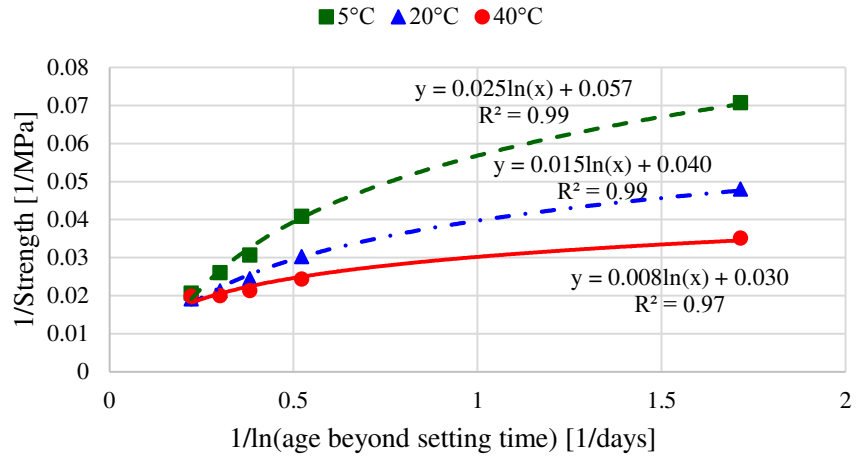


Figure C.1 Reciprocal of experimental strength vs. reciprocal reciprocal natural logarithm of age beyond final setting time at 20°C for Control specimens

T-values at the three temperatures for the proposed method are inverse of coefficients in front of the natural logarithm for each curve in Figure C.1 and the results were summarized in Table C.3.

Table C.3 T-values at each of temperatures in the proposed method for Control specimens

Curing Temperatures [°C]	T-values [-]
5	39.84
20	68.03
40	125.00

To determine  $T_0$ , k-values vs. temperature was plotted as Figure C.2.

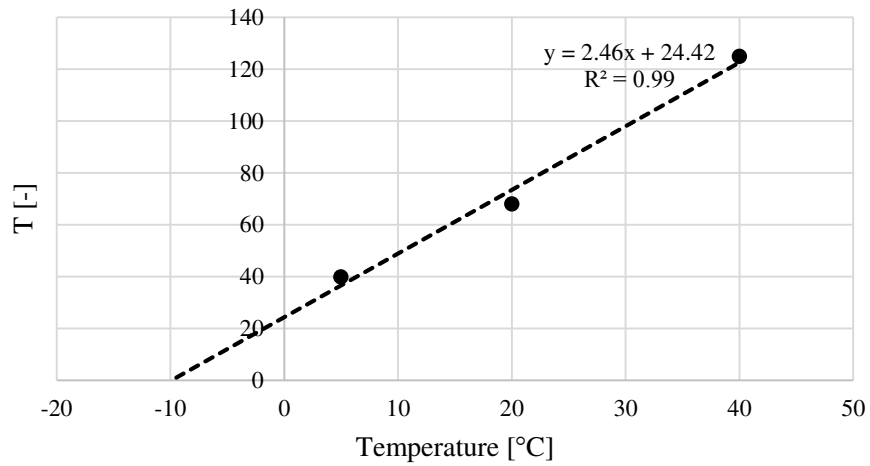


Figure C.2 T-values vs. curing temperature for Control specimen in the proposed method

$T_0$  is the point where the straight line cuts the x-axis. Thus,  $T_0$  for Control in the proposed method is  $-9.94^{\circ}\text{C}$ .

Table C.4 Reciprocal curing temperature and natural logarithm of T-values for Control specimen

1/Curing Temperatures [ $1/^{\circ}\text{K}$ ]	$\ln(T)$ [-]
0.0036	3.69
0.0034	4.22
0.0032	4.83

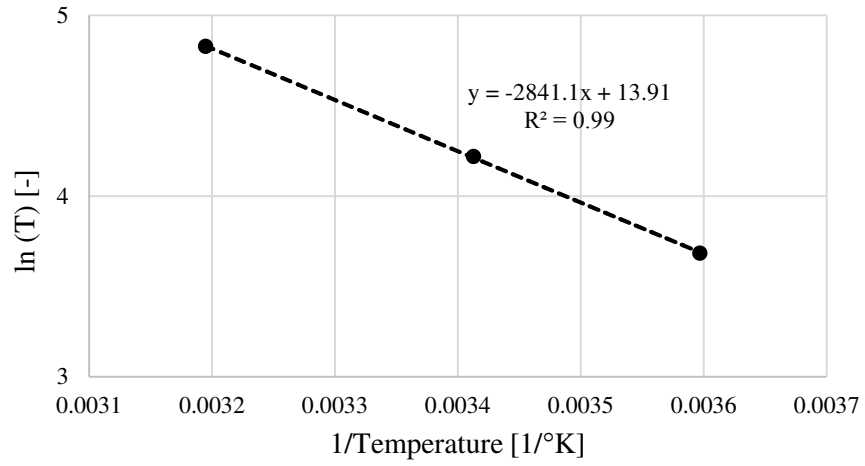


Figure C.3 Natural logarithm of T-values vs. inverse absolute temperature for Control specimens in the proposed method

Slope of the straight line is equal to  $-E_a/R$ , where R is gas constant.  $E_a$  for Control in the proposed method is 23621 J/mol.